NEW METHODOLOGIES FOR ENVIRONMENTALLY FRIENDLY MICROCAPSULE DESIGN

Mattia Collu

UNIVERSITAT ROVIRA i VIRGILI

NEW METHODOLOGIES FOR ENVIRONMENTALLY FRIENDLY MICROCAPSULE DESIGN

Mattia Collu

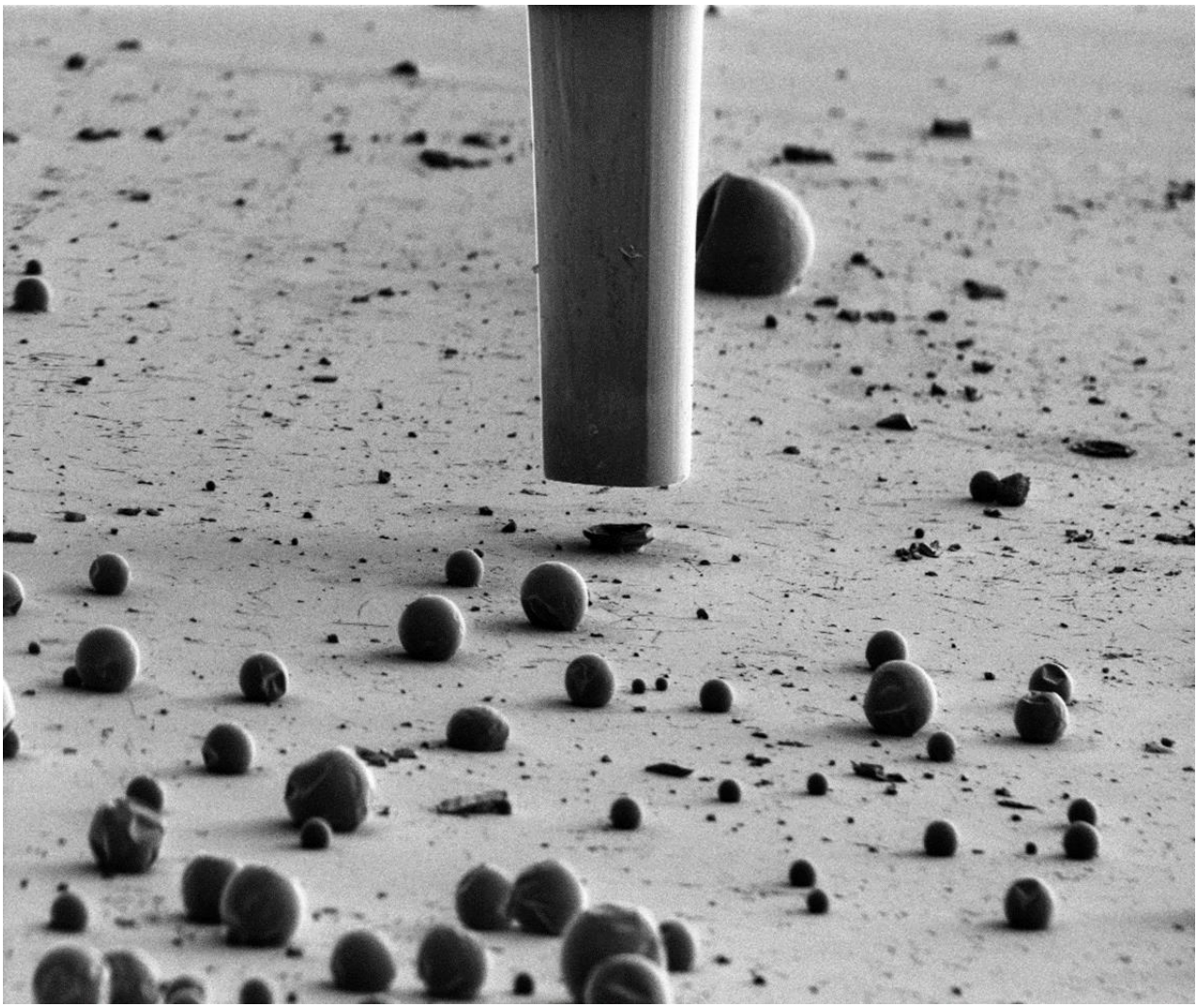

DOCTORAL THESIS
2024

UNIVERSITAT ROVIRA I VIRGILI
NEW METHODOLOGIES FOR ENVIRONMENTALLY FRIENDLY MICROCAPSULE DESIGN
Mattia Collu

Universitat Rovira i Virgili
Procter & Gamble

NEW METHODOLOGIES FOR ENVIRONMENTALLY FRIENDLY MICROCAPSULE DESIGN

by
Mattia Collu

Academic Supervisor
Prof. Marta Giamberini

Company Supervisor
Johan Smets, PhD.

2024

Department d'Enginyeria Química
Campus Sescelades,
Avda. Països Catalans, 26
43007 Tarragona
Tel: 977 55 97 87
Fax: 977 55 96 21

Dr. Marta Giamberini, Associate Professor at the University of Rovira I Virgili, Department of Chemical Engineering.

Dr. Johan Smets, Vice-President, Victor Mills at P&G Brussels Innovation Center

CERTIFY that the present study, entitled "NEW METHODOLOGIES FOR ENVIRONMENTALLY FRIENDLY MICROCAPSULE DESIGN", presented by Mattia Collu for the award of the degree of Doctor, has been carried out under our supervision at the P&G Brussels Innovation Center and the Department of Chemical Engineering at University Rovira I Virgili, and that it fulfils all the requirements to be eligible for the International Doctorate Award.

Tarragona, June 2024

Academic Supervisor

Prof. Marta Giamberini

Company Supervisor

Johan Smets, PhD.

Table of Contents

UNIVERSITAT ROVIRA I VIRGILI
NEW METHODOLOGIES FOR ENVIRONMENTALLY FRIENDLY MICROCAPSULE DESIGN
Mattia Collu

Chapter 1: Sustainable Encapsulation

1.1 Micro-encapsulation

In general, encapsulation is a technology in which benefit agents are surrounded by a coating in order to optimize the stability and the release of the active materia. Microcapsules have usually a spherical size, with a diameter which can range from 1 μm to 1000 μm. Figure 1.1 highlights the microcapsule core material (benefit agent) which is surrounded by the shell.

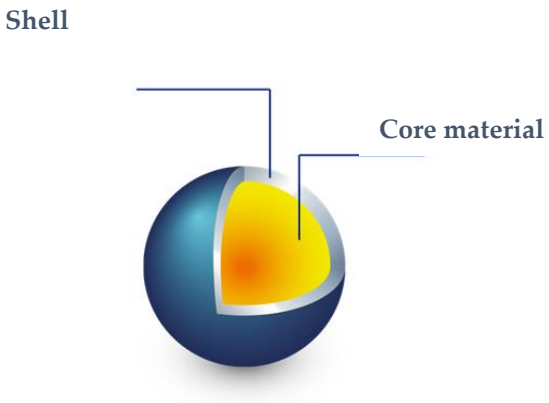

Figure 1.1: Capsule shell which surrounds the core material.

Alike mostly all human inventions, microencapsulation is the result of man's attempt to copy nature. Indeed, examples of microencapsulation can be found in the plants or animals' cells. These natural capsule membranes have the key function of protecting the interior material (core) and control of the flow of materials (permeation) across the cell membrane.

In the late 30's Barret Green started to exploit the encapsulation for carbonless paper. Figure 1.2 represents Green's ink oil phase within a gelatin coacervate: the printing system is then triggered by the pressure of the pen on the paper [1]. When the dye is released, it reacts with the acidic layer on the underside of the sheet.

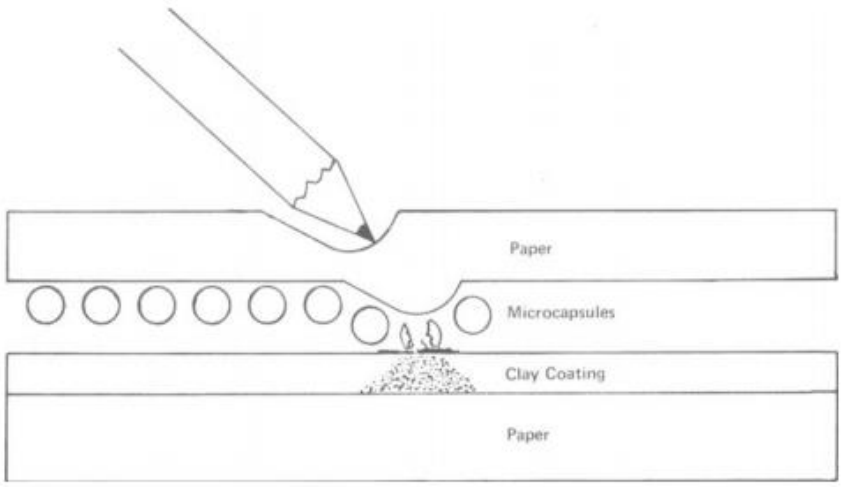

Figure 1.2: Pressure-activated release of encapsulated dye-precursor to give a colour reaction on paper coated with acidic clay, Figure taken from [1].

Generally, the wall material can comprise melamine-formaldehyde [2] to polyurethane [3] and polyurea however the material is strictly correlated to the encapsulation technique. Different materials will be optimal for a specific encapsulation methodology as described in Section 1.1.4.

An alternative to microcapsules are Nanocapsules, which are smaller in size compared to microencapsules. Nanocapsules consist of a core that contains active ingredients and is surrounded by a shell material. The active ingredients are confined within an interior cavity of the nanocapsule, while the shell material encapsulates and protects them. Nanocapsules typically have sizes ranging from 10 to 1000 nanometers [4]. Nanocapsules are extensively used in the pharmaceutical field, they are usually preferred to microcapsules when their subcellular size is needed to enable higher intracellular uptake [5].

1.1.1 Morphology Microcapsules

Microcapsules can be classified into three basic categories as monocore, polycore and matrix types [6] as shown in Figure 1.3.

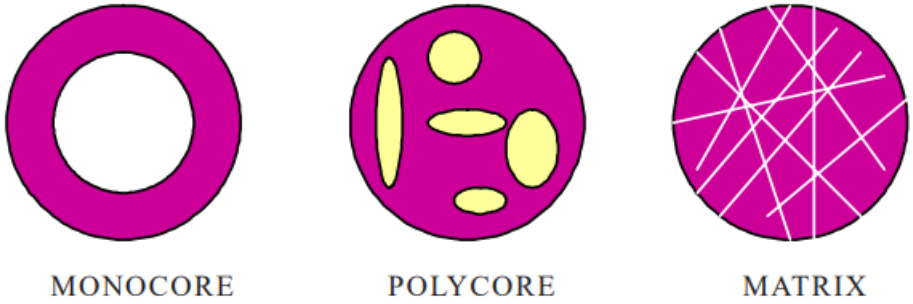

Figure 1.3: Different types of Microcapsules: Monocore, polycore and Matrix [6].

Monocore microcapsules are characterized by the presence of a single hollow chamber enclosed within the capsule's structure. This unique feature allows for the containment and protection of a specific substance within the confines of the capsule.

On the other hand, polycore microcapsules present a more intricate internal architecture. Unlike their monocore counterparts, polycore microcapsules consist of multiple chambers nestled within the shell. These chambers can vary in size, providing opportunities for the encapsulation of different substances or enabling the creation of complex encapsulation systems. The presence of multiple chambers within a single microcapsule opens up possibilities for a range of applications, such as multi-component drug delivery or controlled release of various active compounds.

In contrast to both monocore and polycore microcapsules, matrix type microparticles offer a different approach to encapsulation. In this case, the active ingredients are not confined within chambers, but rather integrated within the matrix of the shell material. This integration results in a homogenous distribution of the encapsulated materials throughout the structure of the microparticle [7].

It is important to emphasize that the design of the microcapsules morphology is heavily influenced by the shell materials and the end-use applications.

1.1.2 Benefit of Microencapsulation

Encapsulation enables the segregation of a core material from its environment for preservation, safety, controlled release, or the enhanced processing, mixing, and handling of a material [8].

Amongst the principal reasons for encapsulation are:

1. Separation of incompatible components

2. Increased stability (e.g. protection of the encapsulated materials against oxidation or deactivation due to reaction in the environment)
3. Masking of odour, taste and activity of encapsulated materials
4. Protection of the immediate environment
5. Controlled release of active compounds (sustained or delayed release)
6. Targeted release of encapsulated materials

Encapsulation offers numerous benefits across various industries and applications. One of the key advantages of encapsulation is the separation of incompatible components. By encapsulating materials, especially those that are reactive or incompatible with each other, their direct contact can be prevented. This separation ensures the preservation of each component's functionality allowing them to coexist in a controlled environment without undesirable reactions or degradation.

Another significant benefit of encapsulation is the increased stability it provides. Encapsulating materials can protect them from oxidation, moisture, light, and other environmental factors that may cause degradation or deactivation. This protective barrier prolonging the active shelf life.

Encapsulation also offers the advantage of masking odors, tastes, and activities of encapsulated materials. This is particularly useful in the food and pharmaceutical industries, where certain ingredients may have strong or undesirable sensory characteristics.

Furthermore, encapsulation contributes to the protection of the immediate environment. Some materials, such as hazardous chemicals or volatile substances, may pose risks to human health or the environment if released or exposed. Encapsulation provides a containment system that prevents release of such materials, minimizing the potential for environmental contamination.

Controlled release of active compounds is another crucial benefit of encapsulation. Through encapsulation techniques, active compounds can be released in a sustained or delayed manner, allowing for targeted delivery and prolonged effects. This controlled release mechanism is particularly valuable in drug delivery systems, where the encapsulated substances can be gradually released in the desired dosage and at the desired rate, ensuring optimal therapeutic outcomes.

Moreover, encapsulation enables targeted release of encapsulated materials. By designing encapsulation systems with specific properties, such as pH-sensitivity or temperature-responsiveness, the release of encapsulated materials can be triggered under specific conditions. This targeted release capability is

particularly advantageous in applications such as drug delivery, where the encapsulated substances can be released at the site of action, enhancing their effectiveness while minimizing side effects. For example, the use of microcapsules allows for the prolonged efficacy of the medication in patients. This, in turn, leads to reduced frequency of administration and enhanced medication compliance [9].

In summary, encapsulation offers a range of benefits, these advantages make encapsulation a valuable tool in various industries as highlighted in Section 1.1.5.

1.1.3 Release Mechanism

Microcapsules offer the ability to release their encapsulated materials in response to specific triggers [10]. These **triggers** can be carefully designed to enable controlled and targeted release, enhancing the effectiveness of the microcapsules in various applications.

One common trigger for the release of active materials from microcapsules is **mechanical forces**. By subjecting the capsules to external mechanical forces, such as compression, shear, or agitation, the capsules can rupture, leading to the release of the encapsulated content [11]. Specifically, Yeo et al. elucidated how, for drug delivery micro-capsules, the rupture load should be optimized for prolonged release of the capsules content, showing how a poor mechanical properties microcapsule results in poor drug release [12]. The mechanical strength of the capsules can be adjusted by modifying the process conditions during production. Mechanical properties will be discussed extensively discussed in Chapter 2:.

Similarly, **Diffusion-based** release mechanisms can be highly effective in certain applications [13]. By tuning the morphology of the capsules it is possible to tune the diffusion coefficients too [14]. For example the pharmaceutical sector frequently relies on the capability to regulate the controlled release of active substances by permeating through the microcapsule shell [15]. This process is contingent upon the diffusion coefficient and solubility of the active ingredient within the barrier [16]. Diffusion can be controlled by tuning parameters such as wall thickness, size of the capsule, porosity and properties of the polymeric network. A thicker shell can help limit leakage by providing a more robust barrier, reducing the chances of the active ingredient escaping prematurely [17]. However, as excessively thick walls can hinder the on-demand release of the active material, finding the optimal shell thickness is crucial to achieve both effective containment and controlled release [18].

The size of the capsule is an important factor that significantly influences the release of encapsulated active [19]. The influence of particle size on the diffusion can be comprehended by considering two

interconnected factors: surface area and shell thickness. When the shell material weight remains constant, smaller microcapsules exhibit a greater surface area. Furthermore, as the particle size decreases, the shell thickness also decreases for a constant core/shell ratio [20]. Moreover, particle size directly impacts the surface area-to-volume ratio, which in turn affects the release kinetics of the microcapsules. When it comes to smaller capsule sizes, the surface area-to-volume ratio increases. So from a theoretical point of view, this higher ratio leads to a larger contact area between the shell and the external environment or the surrounding medium. Consequently, the release process can occur more rapidly due to the increased exposure of the encapsulated material to the external factors. Therefore, smaller capsules generally exhibit faster release rates compared to larger ones, making them suitable for applications where a rapid release is desired. The effect of particle size was assessed by Visscher et al. to understand the degradation rates of poly(D1-lactide-co-glycolide) microcapsules, however no remarkable difference was observed between the size groups examined [21]. Similarly controlling the porosity of the shell helps regulate the diffusion rates of the encapsulated materials [22]. Higher porosity can lead to increased permeability, allowing the active ingredient to escape more easily. Finally, the properties of the polymeric network, such as, chain length, flexibility and mobility, water-uptake and swelling behavior will affect the diffusion rate across the polymeric matrix [23].

pH-sensitive wall materials are frequently employed in pharmaceutical applications. These materials can undergo changes in solubility or permeability in response to variations in pH. For example, the wall may be solid and impermeable at one pH range and become soluble or permeable at another pH range. This pH-dependent behavior allows for precise control over the release of active ingredients based on the specific pH conditions encountered in different environments. pH-sensitive microcapsules have found applications in targeted drug delivery systems, where the release is triggered in specific regions of the body with distinct pH levels. For example, Werner et al synthesized hydrogel membrane microcapsules with reversibly tunable permeation, meaning permeability can be changed by altering pH due to a change in the degree swelling of the membrane [24].

Dissolution is another trigger mechanism commonly used in microencapsulation. It involves the use of coatings that are designed to dissolve under specific conditions, such as immersion in water or exposure to a particular solvent [25]. For example, effervescent tablets often utilize dissolution triggers, where the encapsulated active ingredients remain stable and protected until the capsule dissolves upon contact with the appropriate medium, such as water.

In recent years, significant research efforts have focused on the development of **photosensitive** microcapsules. These microcapsules contain photosensitive moieties that can undergo various photo-induced reactions upon exposure to light. For example, photo-isomerization can cause a change in configuration within the photosensitive moiety, while photo-cleavage can result in the cleavage of the moiety. These light-induced reactions serve as triggers for the release of the encapsulated materials, offering precise control and tunability, such as in the work of Pirone et al [26].

In summary, to achieve the desired release upon specific trigger mechanisms, it is necessary to tailor parameters such as shell thickness, compaction, and capsule size [27].

1.1.4 Microencapsulation techniques

Generally, microencapsulation is characterized by the dissolution of the core and the wall material in specific solvents. The process is divided in two steps: (i) droplet formation and (ii) droplet stabilization. The formation of the droplet is always obtained via dispersion of a liquid in another liquid or in air; the stabilization can be due to chemical reactions (polymerization, crosslinking, coacervation, etc..), solvent evaporation, solvent removal and polymer precipitation, etc. and mainly consists in the formation of the solid external layer.

The droplet formation is characterized by the emulsification process, where an emulsion is a mixture of two or more liquids that are normally immiscible owing to liquid-liquid phase separation. Emulsions are colloidal systems composed of two immiscible liquids. These liquids are dispersed as tiny droplets throughout the system. The dispersed phase refers to the droplets of one liquid suspended within the other liquid, known as the continuous phase. The interface, in this context, refers to the region where the dispersed and continuous phases meet and interact with each other [28].

Microencapsulation techniques have been extensively studied and can be broadly categorized into two main groups: Chemical methods and Physical/mechanical methods [29]. Chemical methods encompass methods that employ monomers/prepolymers as starting materials, involving chemical reactions. Conversely, Physical/mechanical methods comprise methods that utilize polymers as starting materials, where shape fabrication occurs without any chemical reactions taking place.

1.1.4.1 Physical Mechanical methods

1.1.4.1.1 Spraydrying

Spray drying, is a technique employed to transform a liquid product into an instantly obtainable powder by atomizing it in a stream of hot gas [30]. As shown in Figure 1.4, Spray-drying starts with the emulsion of the active component in water or an organic solvent followed by a drying process.

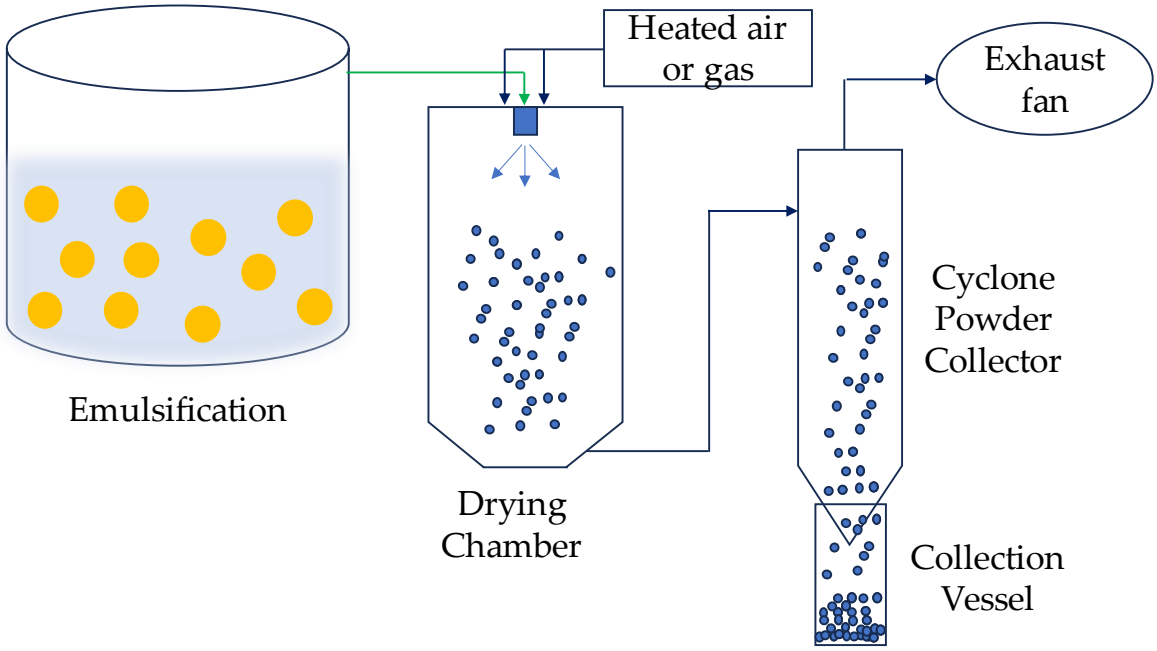

Figure 1.4: Schematic representation of encapsulation of oil core via Spray drying.

Figure 1.4 illustrates the process where the oil-in-water emulsion enters the drying chamber, which is heated either by air or, in some cases, an inert gas. The emulsion undergoes atomization as the solvent evaporates, leading to the solidification of the shell material around the core material droplets. Once dried the particles are separated and collected into the *cyclone powder collector*.

Depending on the starting feed material and operating conditions, spray-drying can yield either a very fine powder (10–50 μm) or larger particles (2–3 mm) [31].

Spray-drying is widely utilized in engineering practices to remove water from solutions. In the food industry, it is commonly employed to achieve microbiological stability, mitigate the risk of chemical or biological degradation, reduce storage and transportation costs, and obtain products with specific properties, such as instantaneous solubility [31]. One drawback associated with this method, particularly

when encapsulating volatile substances like fragrances, is the requirement for the chamber to be heated in order to facilitate water evaporation. Unfortunately, this heating process inadvertently leads to the evaporation of a portion of the fragrance as well, resulting in suboptimal encapsulation efficiency [31].

Carbohydrates, including starch and maltodextrins (starch hydrolysates) [32], proteins such as whey protein and sodium caseinate [33], lecithin, and gums like Gum Arabic, are extensively investigated as wall materials for spray-drying [34, 35].

1.1.4.1 Chemical methods

Chemical microencapsulation methods leverage various techniques, such as interfacial polymerisation [36], in situ polymerisation [37].

1.1.4.1.1 Coacervation

The method of **coacervation** comprises the phase separation of a polymer-rich phase (coacervate) and a polymer-poor phase (the coacervation medium). The term "coacervation" derives from the Latin word "acervus," meaning aggregation, and the prefix "co" signifies the fusion of colloid particles [38]. This process involves the hydrocolloid separating from the primary solution and subsequently aggregating into a distinct, liquid phase known as "coacervate" [39].

Microcapsule formation via coacervation can be categorized into two types: simple and complex coacervation. Simple coacervation utilizes a single polymer in either aqueous or organic media, respectively. In contrast, complex coacervation involves the interaction between two oppositely charged polymeric materials. Simple and Complex coacervation are represented in Figure 1.5.

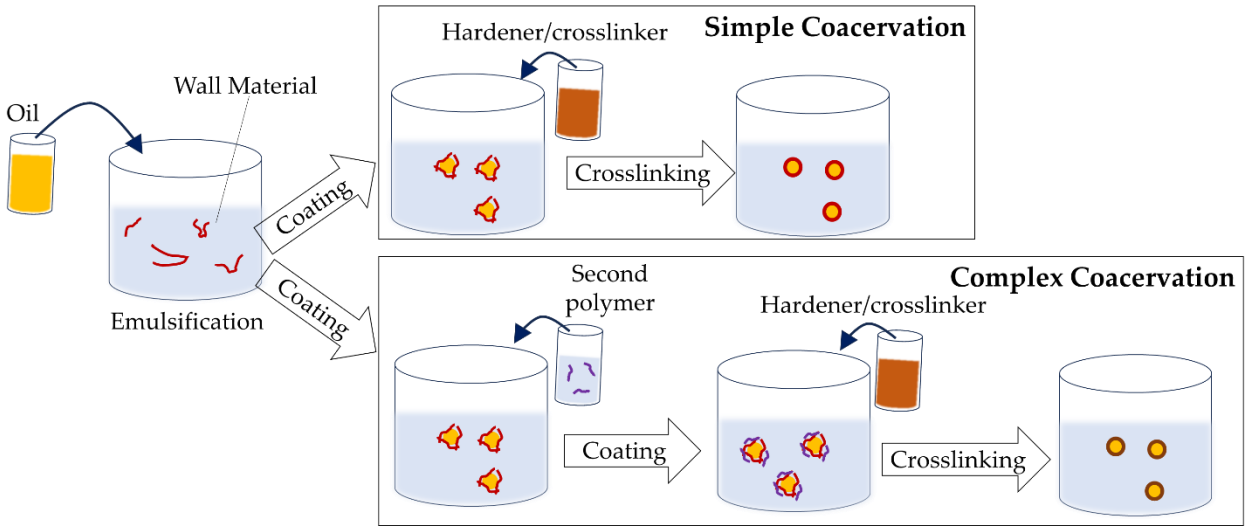

Figure 1.5: Representation of encapsulation of oil core via simple and complex coacervation [40].

As shown in Figure 1.5, coacervation commences with the emulsification of the core material into the continuous phase, which contains the wall material. The encapsulating material is then induced to precipitate as a coacervate onto the encapsulated material through various methods.

In the context of simple coacervation, a singular polymer is precipitated around the core material. This is accomplished by thermodynamic change of state that prompts the desolvation of the shell wall material. This change of state, such as alterations in pH or temperature, cause deposition of the coacervate phase around the droplets of the active ingredient. These modifications may be induced by the introduction of electrolytes (e.g., sodium sulfate), the addition of a water-miscible solvent (like ethanol), or temperature adjustments, either raising or lowering it [41, 42].

On the other hand, complex coacervation is triggered by the neutralization of two polymers bearing opposite charges. The primary driving force behind complex coacervation lies in the reduction of the free electrostatic energy, resulting from the interaction between ions of opposing charges [43]. This process is further influenced by a multitude of parameters, including pH, ionic strength, the nature of the core material, and the ratio of core to wall constituents [44]. In both variants of coacervation, be it simple or complex, the ultimate step can involve the reaction between the cross-linking agent and the coacervate.

The type of wall material can comprise cellulose materials (ethylcellulose, hydroxyl propylmethyl cellulose, sodium carboxy methyl cellulose), sodium alginate, PLGA, gelatine, polyesters, chitosans, etc [45]. Notably, gelatin-Arabic gum proves to be the most commonly employed system for complex coacervation [46].

1.1.4.1.2 Interfacial polymerization

In **interfacial polymerization**, the polymer microcapsule shell is formed through the polymerization of monomers at the interface of two immiscible phases (mostly liquid-liquid). The continuous aqueous phase contains the hydrophilic monomer, while the dispersed phase within the oil droplets accommodates the hydrophobic monomer.

As shown in Figure 1.6, one of the monomers is combined with the benefit agent prior to emulsification. The shell is then formed by the reaction of monomers at the interface.

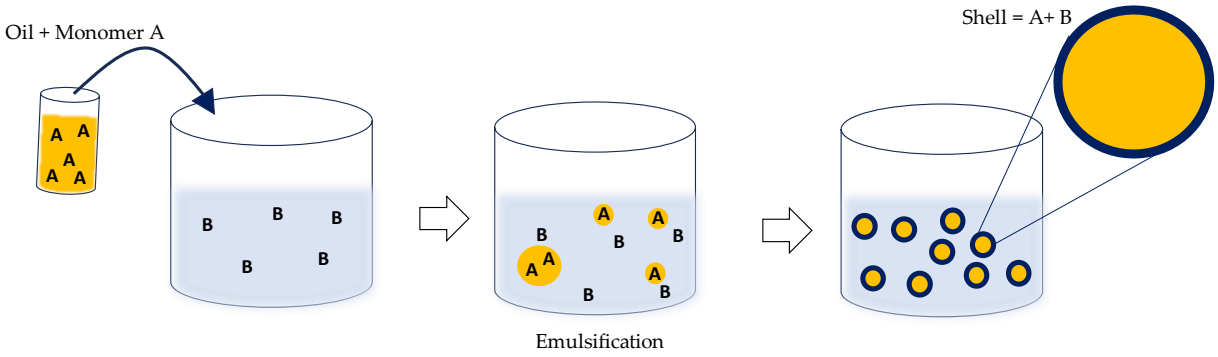

Figure 1.6: Schematic representation of encapsulation method via interfacial polymerization.

Precisely at the interface of the two phases, polymerization is initiated by the interaction of the monomers with the initiators. Polymer chains start to form and grow, leading to the formation of a polymer shell around the core droplets. Firtstly polymerization takes place at the interface, governed by chemical kinetics. This rapid polymerization forms a thin film. Once the polymer reaches a certain molecular weight it migrates to the interface to thicken the polymer wall from inside the microcapsule [47]. As time passes, the increasing thickness of the polymer film leads to slower polymerization controlled by monomer diffusion. Eventually, the reaction stops due to diffusion barriers. Therefore, the film thickness initially grows rapidly, but the rate diminishes over time, reaching a maximum [48].

A drawback of interfacial polymerization lies in the fact that the restricted solubility of specific fragrance constituents in water has the potential to disturb the course of interfacial polymerization, thereby leading to the possibility of these perfume elements reacting with monomers and ultimately causing modifications in the fragrance composition [49].

The wall materials generated by interfacial polymerization include polyamides, polyimides, polyesters, polyamines, polyurethanes [48]. For example, a polyurethane shell is achieved such as in the work of

Saihi which produced microcapsules by the interfacial polymerizatoin of diphenyl methylene diisocyanate, MDI (dissolved in toluene) and water at the interface of drops of the aqueous phase (containing DAHP) dispersed in the organic phase [50].

1.1.4.1.3 In-Situ polymerization

The **in-situ polymerization** process consists of the dispersion of one phase containing a reactive monomer into a second immiscible phase [7]. The main difference with the interfacial polymerization is that all reactants are included in one single phase of the emulsion, continuous or discontinuous. Therefore the polymerization takes place in the phase which contains the monomers.

As represented by Figure 1.7 there can be two cases of insitu polymerization: either monomer is located in the discontinuous phase (box A of Figure 1.7) or the monomer is in the continuous phase (box B of Figure 1.7).

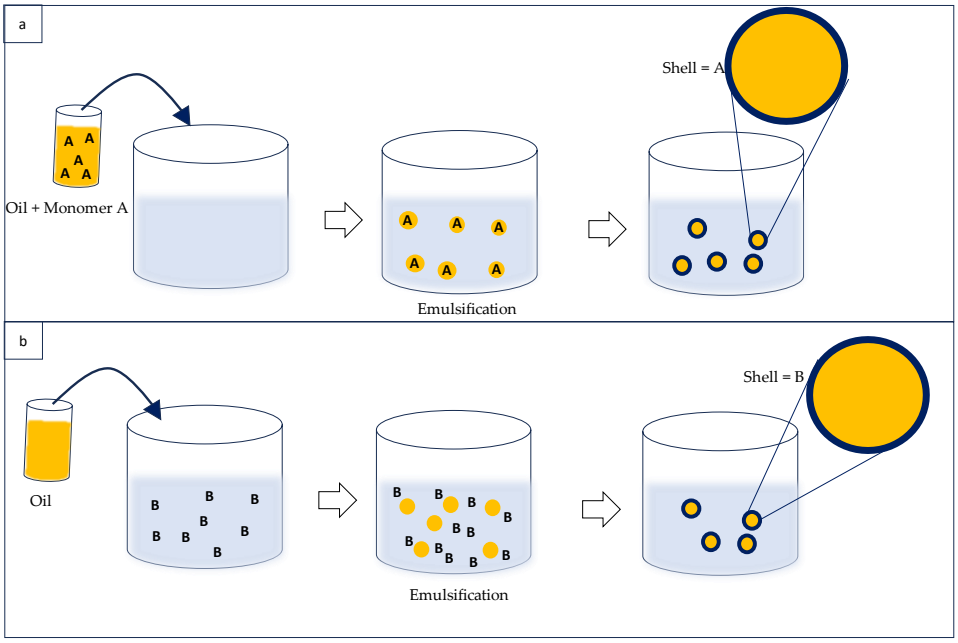

Figure 1.7: Schematic representation of encapsulation via in situ polymerization method, Example of in-situ polymerization where the monomer is located in the discontinuous phase (box a), monomer is in the continuous phase (b).

Following the emulsification process, the polymerization takes place, the monomers first forms a low molecular weight prepolymer and, as the prepolymer grows, it migrates and deposits on the interface of dispersed phase, resulting in formation of microcapsules.

In-situ technique is often preferred for being easier to perform, relatively simpler to scale up, though the synthesis is often longer compared to other procedures [51].

Among the most common materials for in-situ polymerization are urea formaldehyde and melamine formaldehyde [2].

Lastly **PAC** (Poly Acrylate Capsules), the microcapsules market reference of this work, which will be described extensively in Section 2.2.2.1, are made by leveraging in-situ polymerization.

1.1.5 Applications

Encapsulation technology has been widely utilized in various industrial applications in recent years due to its ability to provide controlled release. In each of these fields, different types of capsules have been developed to meet the specific requirements of each application. The following section aims to provide an overview of these developments.

Firstly microcapsules have gained significant attention in **pharmaceutical** research due to their ability to provide controlled release, enabling precise and targeted drug delivery. Moreover, microcapsules serve as a protective barrier for active pharmaceutical ingredients, shielding them from external factors. However, biocompatibility remains a significant concern, as interactions between microcapsules and biological systems could give rise to immune responses or toxicity issues. Therefore, thorough measures must be taken to address these concerns and ensure patient safety. Several scientific teams have directed their attention toward harnessing the potential of encapsulation in acting as carriers for drug delivery. As an exemplification, Vishnu et al. [52] employed alginate-based capsules to encapsulate Verapamil hydrochloride, a medication utilized for managing hypertension. In a similar manner, Wang et al. [53] formulated microcapsules loaded with carvacrol, which were specifically designed to target the intestines and enhance antimicrobial efficacy while also boosting bioavailability. Their investigation revealed that less than 20% of the active was released in the stomach, with the remaining portion being completely discharged in the intestines.

Secondly encapsulation serves as a valuable technology within the **food** industry, offering a range of benefits. It provides a protective barrier for sensitive ingredients, such as vitamins, antioxidants, while also it can mask unpleasant odors and tastes. For instance, in a scientific study by Majeed et al. [54], the encapsulation of essential oils was explored for the purpose of protecting and precisely releasing them in food applications. Similarly, Gomes et al. [55] conducted research on Poly (DL-lactide-co-glycolide) Nanoparticles loaded with trans-Cinnamaldehyde and Eugenol. The aim was to employ these encapsulated compounds for antimicrobial delivery to inhibit the growth of foodborne pathogens such as Salmonella and Listeria.

Furthermore, black seed oil possesses therapeutic benefits, albeit accompanied by an unpleasant taste. To address this, Alkhatib et al. [56] devised a method of encapsulating black seed oil in alginate microcapsules, effectively masking the taste and enhancing palatability.

Moreover, encapsulation technology plays a pivotal role in the **agriculture** industry. It provides a protective shield for sensitive agricultural inputs, such as pesticides, fertilizers. Moreover, by encapsulating nutrients or bioactive compounds, their release can be regulated, allowing for a sustained and targeted delivery to plants or soil. Various studies highlighted the successful utilization of encapsulation in the agricultural industry. In a study conducted by Yu et al. [57] capsules were synthesized using chitosan and methylene diphenyl diisocyanate (MDI) via interfacial polymerization, where the encapsulation of a pesticide agent achieved an encapsulation efficiency of 93.3%. Similarly, Cote et al. [58] employed biopolymers such as potato starch combined with rice flour, rye, barley, and soybean powders to create capsules. These capsules were utilized to encapsulate an insecticidal agent, resulting in an extended duration of mortality for Choristoneura rosaceana, an insect that inflicts damage on fruit crops. The application of the encapsulation formulation demonstrated promising results in controlling the population of this pest.

Lastly, In the field of **cosmetic** formulations, microencapsulation serves as a valuable strategy to safeguard fragrances and active agents against detrimental effects caused by heat, light, moisture, and interactions with other substances over an extended shelf life. Additionally, microencapsulation precise control of the release rate [59]. For reference, in a study conducted by Kim et al. [60], capsules were fabricated using polylactic acid to encapsulate retinyl retinoate, a compound renowned for its anti-wrinkle properties. The encapsulated agent exhibited a higher efficacy in reducing facial wrinkles compared to the non-encapsulated formula, highlighting the enhanced performance achieved through microencapsulation.

In summary perfume microcapsules have been developed in numerous consumer good products such as Shampoo compositions [61], conditioners [62] and deodorants [63] in order to increase the deposition and retention of benefit agent, however .The focus of these work would be in developing microcapsules for detergents applications.

1.1.5.1 Fragrance encapsulation in Laundry detergents

Fragrances are complex mixtures containing blends of aroma compounds such as essential oils or synthetic molecules [64]. When these fragrance molecules are released, they engage with olfactory receptors in the human sensory system, initiating the subsequent processing of this sensory input as perception within the cerebral domain of the brain [65]. The perception and detectability of fragrant molecules rely on the activation thresholds of their corresponding olfactory receptors, situated on specialized neurons responsible for olfaction. These activation thresholds represent the minimum concentration of a fragrant compound required to evoke a noticeable response under standardized conditions [65].

Notably, even a slight alteration in the chemical composition of a compound can result in a complete change of its scent profile [34]**.**

Fragrance chemicals find their way into various consumer products, such as laundry detergents, fabric softeners, soaps, and personal care items like shampoos, body washes, deodorants, and numerous others. The inclusion of aroma in these products serves to provide a pleasing scent and contribute to uplifting emotional states [66].

Specifically, perfumes are created by blending aromatic ingredients to create a desired scent profile. These scents are categorized into top notes, middle notes, and base notes. Top notes make the initial impression, with high volatility and a strong impact. Middle notes add body and fullness with intermediate volatility. Base notes, having low volatility, evaporate slowly, ensuring a long-lasting scent.

As it can be seen from Figure 1.8 the balance between top, middle and bottom notes depend on the specific application of the perfume fragrance.

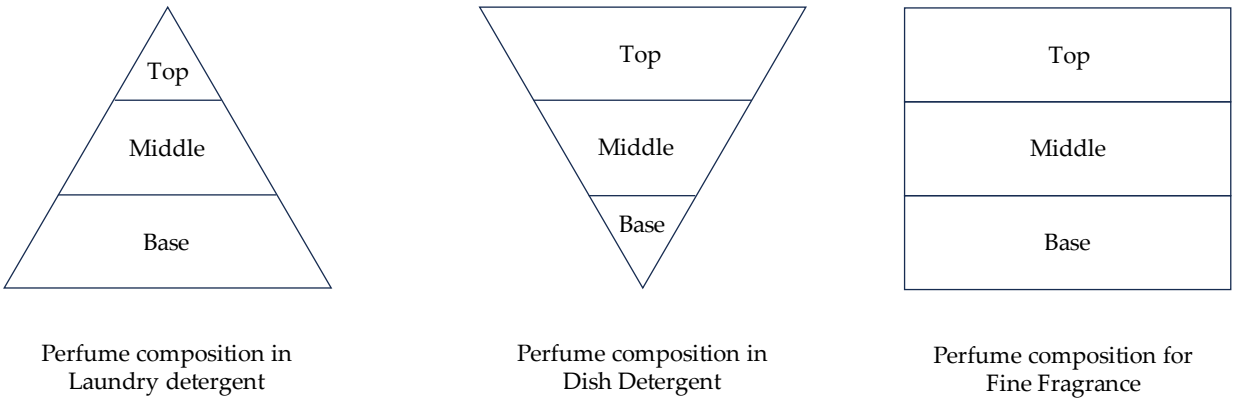

Figure 1.8: Structure of perfumes in terms of Top, middle, base notes based on the application of the perfume.

The purpose of perfume in laundry detergent is to deliver a lasting scent to fabrics, ensuring that it lingers even after use. To achieve this, the perfume is formulated with a higher concentration of base notes and lower volatility, ensuring a longer-lasting fragrance. On the other hand, dish detergent fragrances are designed to bloom while washing dishes but not remain long on the dishes. Therefore, these fragrances contain a higher proportion of top notes, providing a burst of scent during use. In contrast, fine fragrances strike a balance between top, middle, and base notes for a harmonious composition.

However, incorporating fragrances directly into laundry products presents several challenges. Firstly, a significant amount of perfume is lost during the washing cycles instead of depositing on fabrics. Additionally, the high volatility of the fragrances results in limited longevity of the scent on treated fabrics [67]. Lastly, the chemical instability within product formulations [67] [68] greatly reduces the effectiveness of the active ingredients, especially when considering that the product may be stored for up to 18 months before usage [69].

To address abovementioned challenges, microencapsulation of fragrances has emerged as a promising technique. By isolating the fragrance core from its surroundings, microencapsulation enhances fragrance stability and enables controlled release [70].

In Figure 1.9 examples of fabric care products utilizing perfume microcapsules to enhance consumer satisfaction are showcased. These microcapsules contribute to an elevated sensory experience.

Figure 1.9: Household Products comprising microcapsules.

Chapter 2: Capsule performance

Abstract

In the field of encapsulation, microcapsules containing perfume have emerged as effective vehicles for delivering active ingredients across various applications. The present study employed a multivariate analysis framework to examine polyacrylate microcapsules for household products synthesized using different acrylate monomers.

Leveraging the *Wall Film* model system, the micro-capsules were synthesized via in-situ polymerization, using varying concentrations of three acrylate monomers: CN975(Aromatic Hexafunctional Urethane Acrylate),CM6 (Dipentaerythritol penta-/hexa-acrylate) and M8 (1,2-(triglycolate diacrylate)ethylene glycol)).

The advanced multivariate approach allowed us to quantify critical features such as the Molecular Weight between Crosslinks (MWc), mechanical properties, Encapsulation Efficiency (EE), and On-fabric Delivery. It is worth noting that mechanical properties were gauged using a novel Nanoindentation technique, which measures the Rupture Force per unit diameter (RFD). Both Encapsulation Efficiency and On-fabric Delivery were assessed using GC-MS. Our results identified the optimal microcapsule system as the one synthesized with 100% Aromatic Hexafunctional Urethane Acrylate, show-casing a 94.3% Encapsulation Efficiency and an optimal RFD of 85 N/mm. This system achieved an exemplary On-Fabric delivery rate of 307.5 nmol/L.

This research provides crucial insights for customizing microcapsule design to achieve peak delivery efficiency. Furthermore, by designing acrylic monomers appropriately, one can potentially reduce the amount of active ingredients used, owing to enhanced delivery efficiency and the optimization of other microcapsule properties. Such advancements pave the way for more environmentally friendly and sustainable production processes in the fast-moving consumer goods industry.

2.1 Introduction

Efficient perfume microcapsules rely on optimal mechanical properties since the content is released given a mechanical trigger, resulting in capsule rupture [110]. Hence optimal mechanical properties are

necessary to facilitate the release of the core material precisely at the desired target. The capsules must strike a balance: they must be robust enough to withstand processing and the spinning cycle of a washing machine, yet not excessively strong to prevent the rupture and release of the perfume once the capsules are deposited into the fabrics.

The objective of core–shell systems is the protection of the encapsulated substance from the environment, and its controlled and targeted release. Among the different factors that induce the release in this case the focus is on the mechanical pressure.

Generally, research in microencapsulation has focused on developing novel encapsulation techniques and materials, such as vitamins or cells, while other research focuses primarily on mechanical characterization.

The wall material's molecular structure influences mechanical properties and encapsulation efficiency. Joythi et al. reviewed the various factors affecting the encapsulation efficiency, showing that this performance index depends upon different factors like concentration of the polymer, solubility of the polymer in solvent, rate of solvent removal, solubility of organic solvent in water, etc. [111]. Several literature studies focused on the role of the wall material and its microstructure on the mechanical performances of the system. To the latter, Vinogradova demonstrated how filled microcapsule systems reveal a more decadent mechanical behavior than hollow capsules, showing the crucial role of the osmotic coefficient for the filler [112]. Radtchenko confirmed the finding of Vinogradova, adding that the shell properties entirely control the investigated elastic behavior of filled polymer micro-capsule and highlighting how filled capsules are always softer than hollow ones [113].

Other studies controlled the composition of the wall of the microcapsule: specifically, Rata et al. showed how the cross-linking density of (PVA)-based microcapsules ultimately influences the Swelling Capacity and the encapsulation efficiency, being the capsules with the highest cross-linking density having the lowest Swelling Capacity and encapsulation efficiency [114]; Adding to Rata's work, higher cross-linking is found to improve the stiffness of the capsules [115, 116, 117, 118]. Specifically, Yeo et al. elucidated how, for drug delivery micro-capsules, the rupture load should be optimized for prolonged release of the capsules content, showing how a low polymer concentration results in high internal porosity, poor mechanical properties and thus poor burst for drug release [12]. With this considered, the successful deployment of microencapsulated perfumes strongly relies on their mechanical properties, significantly impacting their delivery efficiency.

Therefore, understanding the mechanical properties of microcapsules is crucial for their behavior in manufacturing and end-use applications. Gray et al. reviewed most of the state-of-the-art experimental techniques for analyzing properties of microcapsules [119], which namely consist of (i) optical tweezers, (ii) shear flow (spinning drop apparatus), (iii) micropipette aspiration, (iv) micromanipulation [118] and (v) atomic force microscopy (AFM) [120]. These methodologies generally use complex compression geometries to obtain information about the microcapsules' elastic (upon contact), elastoplastic (deformation energy), and failure behaviors, providing the **rupture force** and **fractional deformation at rupture**. Moreover, mathematical solutions, including finite element modeling (FEM) aided via experimental validation, have been used to extrapolate stress-strain relationships for the membranes in core-shell structures and extract intrinsic material properties.

In a notable work, R. Mercadé-Prieto et al. proposed a methodology for calculating the rupture stresses of microcapsules under compression testing [122]. By employing finite element modeling and analyzing the critical stresses within the microcapsule wall at various levels of deformation, failure stresses for tetraethoxyorthosilane-methyltrimethoxysilane (TEOS-MTMS) microcapsules with a model core oil were determined. The obtained failure stress values, ranging from 11 to 14±10 MPa, were further analyzed using Weibull distributions. Additionally, insights into the creation of microcapsules and the experimental setup for compression testing were provided, presenting a comprehensive approach to mechanical characterization and failure stress estimation.

Some authors, moreover, investigated the coupled effects of encapsulation and mechanical properties for specific polymeric core-shell systems. Valuable examples include, for instance, the work from Fernandes et al., who highlighted how the release of encapsulated perfume dye was demonstrated to be a function of deformation [124], and Su et al., who investigated Young's modulus and hardness of microcapsules within loading ranges that did not exceed the 'yield point' or 'rupture point' [125].

While this plethora of studies are available, the **connection between the chemical structure and the mechanical properties of the capsule wall has received comparatively less attention**. Indeed, a comprehensive understanding of the **relationships between the molecular structure of the capsules and their mechanical properties and performance remains a crucial research gap**.

To achieve this objective, various acrylate monomers were utilized individually and in combination to achieve capsule walls differing in chemical structure. The mechanical properties, encapsulation efficiency, and performance characteristics of the newly developed capsule systems are thoroughly examined. In the

article, we aim to establish correlations between the molecular structure and the mechanical properties of the microcapsules, particularly in terms of their release efficiency in consumer goods products such as Liquid Fabric Enhancers.

Regarding the mechanical properties characterization, traditional compression methods developed for microcapsule are characterized by intrinsic limits that comprehend both a limited statistical reliability, a poor sensitivity to stiffer micro-capsule systems (the compliance of the actuation cantilever traditionally limits AFM systems), and, ultimately, by the lesser capability to simultaneously span through various particle sizes, providing insights into the multi-scale response of the material systems. Therefore, in the present study, we report an innovative characterization workflow employing nanoindentation at the microscale to fill the abovementioned gap for acrylate-based capsules precisely. Nanoindentation is a powerful technique for characterizing the mechanical properties of polymers at small length scales [127]. Moreover, it can offer a fast and reliable one-degree-of-freedom (d.o.f.) system that allows measurement of rupture properties of single capsules at high throughput toward the industrial exploitation of methodologies [150]. This technique allows applying highly resolved loads to hollow polymeric systems and measuring the force required to break the capsules. The high throughput ultimately enables the testing of several chemically optimized systems.

To the best of the authors' knowledge, very few literatures works employed nanoindentation to study the mechanical behavior of micro-capsules and their rupture under compression—among them, Ghaemi et. Al [151] characterized the deformation of single-filled micro-capsules made of melamine-formaldehyde to study the mechanisms of failure under compression (with the help of FEM simulations) and the release of perfume oil for powder detergents.

2.2 Materials & Methods

2.2.1 Materials

In the context of the synthesis of microcapsules, the commercially available monomers CN975, Dipentaerythritol penta-/hexa-acrylate and 1,2-(oligoglycolate diacrylate)ethylene glycol (herein referred to as CM6 and M8, respectively), were used as purchased without any further purification. Sarton Americas provided monomer A; Sigma-Aldrich provided Monomer CM6, while Monomer C was

synthesized by Ecosynth (Belgium). 2,2′-Azobis(2-methylbutyronitrile)(Vazo™ 52), 2,2′-Azobis(2-methylpropionitrile) (Vazo™ 67), 4,4′-Azobis(4-cyanovaleric acid), isopropyl myristate (IPM), polyvinyl alcohol (PVA) (85,000-124,000 g/mol) were provided by Sigma Aldrich.

Fragrance mixture A, consisting of a mixture of perfume raw materials with a volume-weighted average logP of 3.4 were provided by The Procter &Gamble Company (Strombeek Bever, Belgium).

2.2.2 Methods

2.2.2.1 Microcapsule preparation via in-situ polymerization

The acrylate monomers employed are listed in Table 2.1 together with their MW and the average number of acrylate moiety per molecule. As previously explained, Monomer CN975 consists of an aromatic hexafunctional urethane acrylate, Monomer CM6 is Dipentaerythri-tol pentaacrylate, while Monomer M8 is 1,2-(triglycolate diacrylate)ethylene glycol.

Table 2.1: Chemical structures and MW of Acrylate Monomer employed.

Name	Structure	MW [g/mol]	# Acrylate Moiety
CN975	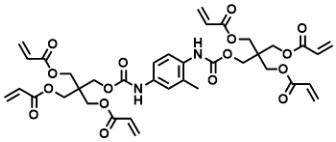	**770**	**6**
CM6	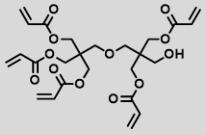	**578**	**5**
M8	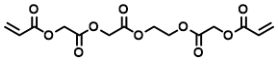	**344**	**2**

The capsules were synthesized via an in-situ polymerization process [81], which consists of the dispersion of one phase containing a reactive monomer into a second immiscible phase [7]. Hence, two immiscible phases were prepared: a Water Phase and an Oil Phase, as shown in Figure 2.1, which represents an overview for the encapsulation process.

A preliminary oil phase, consisting of 42.9 g of fragrance mixture A and 5.84 g of the acrylate monomer mixture reported in *Table 2.3*, which are mixed until the monomer is fully dissolved. A second oil phase

consisting of 26.9 of Fragrance mixture A, 50.21 g isopropyl myristate (IPM), 1.8 g of oil soluble initiators (precisely 1.0 g 2,2′-azobis[2-methylbutyronitrile], and 0.8 g 4,4′-2,2′-Azobis[2-methylpropionitrile]) is prepared separately and mixed until complete homogenization. The two oil phases are then mixed with an overhead stirrer Eurostar 200 digital from IKA (500 rpm) via 90 degrees 4 blades stirrer [81].

The water phase, containing 178.6 g of a 2% water PVOH solution, 0.67 g of the water-soluble initiator (4,4′ -azobis[4-cyanovaleric acid]), and 0.79 g of 21.5% NaOH, was prepared and mixed via IKA Eurostar power control visc E20-MX-1 at 3000 rpm until the 4,4′ -azobis[4-cyanovaleric acid]dissolves.

The water phase was added to the oil phase, and high shear agitation was applied to produce an Oil in Water (O/W) emulsion via an overhead stirrer Eurostar 200 digital from IKA (1200 rpm) via 90 degrees 4 blades stirrer for 30 minutes. The emulsion was included in a Glass Jacketed Flask Reactor Vessel of 500 ml equipped with a reflux condenser and overhead anchor stirrer. The temperature was increased to 75° C in 30 minutes, held at 75° C for 4 hours, increased to 95° C in 30 minutes, and held at 95° C for 6 hours. Finally, the batch was allowed to cool to room temperature. As a result, a population of microcapsules dispersed into the aqueous phase was obtained which is herein defined as capsule slurry.

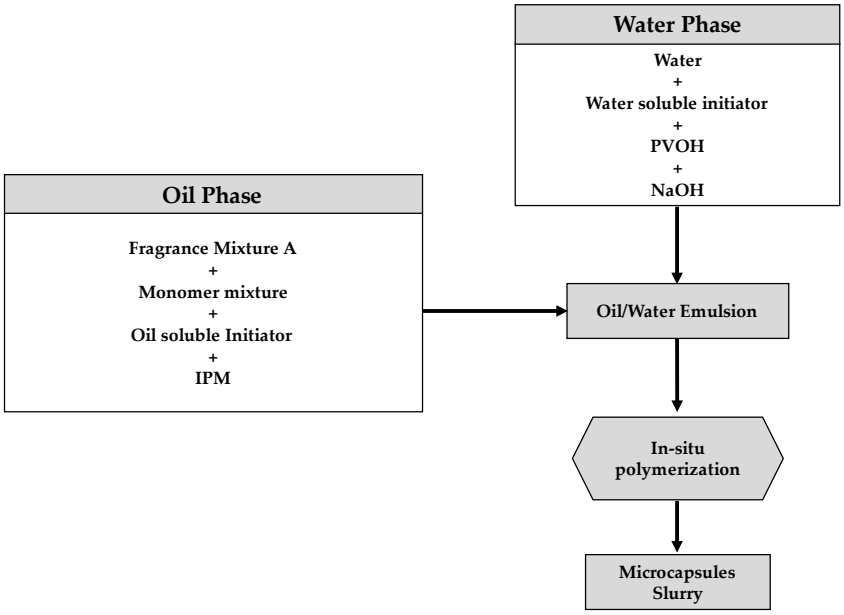

Figure 2.1: Workflow for the synthesis of Microcapsules via in-situ polymerization.

Differently from the procedure described in Procter&Gamble patent [81], no monofunctional monomers were employed. Monofunctional monomers such as (tert-Butylamino)ethyl methacrylate and 2-

Carboxyethyl acrylate are useful to limit the number of unreacted acrylates at the end of the preparation: in fact, the lower Molecular Weight (MW) enables them to diffuse more easily during the formation of the wall, enhancing the overall wall reactivity. Another effect of employing the moofunctional monomers is that the monofunctional monomers can alter the mechanical properties of the wall. In general, by reducing the chain length between crosslinks the deformability of the polymer reduces [152]. This is mostly true, unless the presence of additional factors may modify the overall effect and contribute to variations in the material's behavior such as differences in hydrogen bonding and ring–ring coplanarity. However, to limit the number of variables, monofunctional monomers were not employed in order to simplify the correlation between the chemical structure of the wall and its performance.

As represented in Figure 2.2, the wall growth occurs within the oil phase, as the monomer is a component of the oil phase. The in-situ polymerization approach provides a unique and potentially more effective means of achieving desired encapsulation outcomes than traditional interfacial polymerization commonly documented in the scientific literature, where the monomer is typically present in the water phase [9]. Within this specific process, the mass transfer of the acrylate monomers to the water/oil interphase is essential for successful encapsulation. Hence the role of IPM is vital to optimize the partition coefficient of the core materials and, as a result, improve the mass transfer of monomer to the interphase.

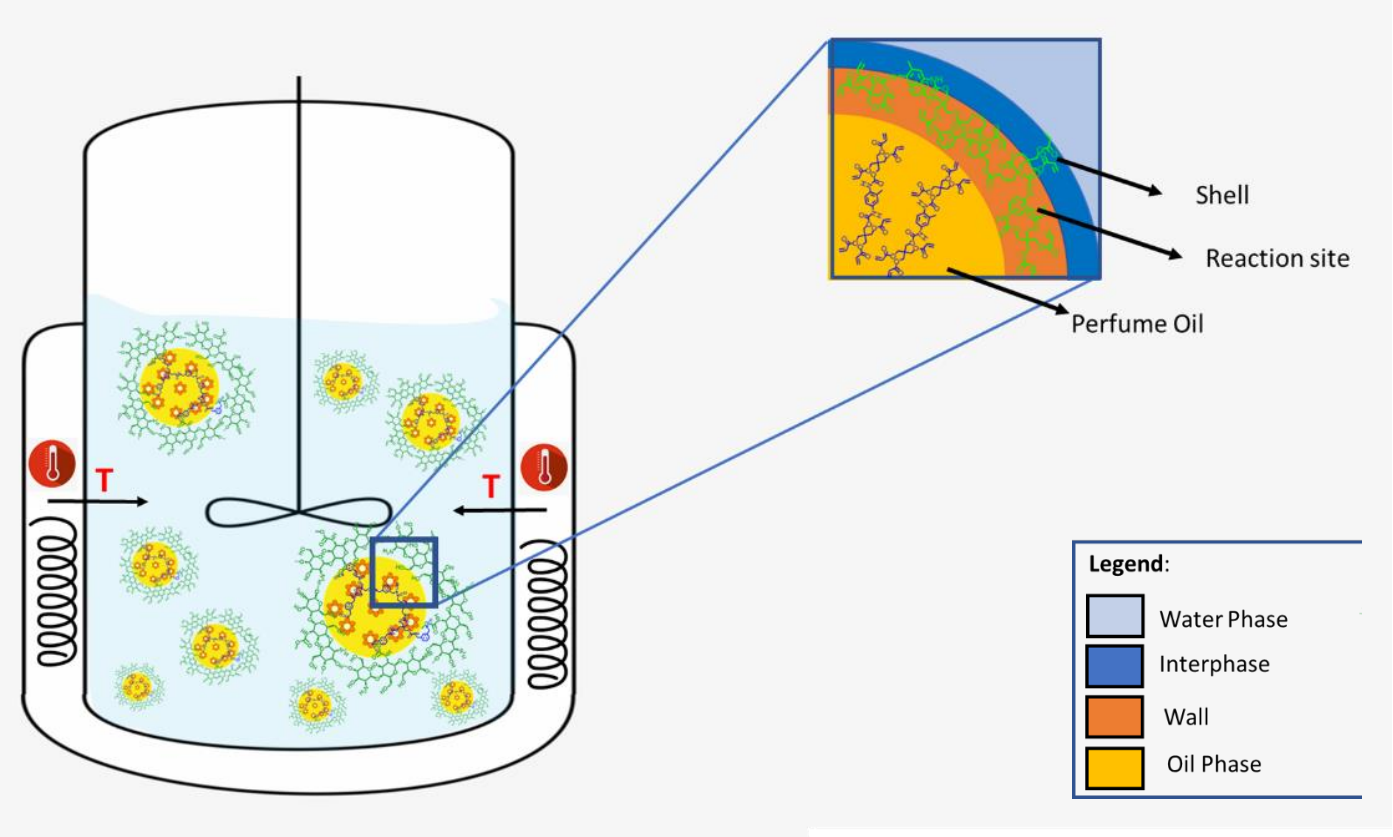

Figure 2.2 Schematic of the in-situ polymerization step.

Polymerization is controlled by the reaction kinetics, which is faster compared to diffusion of monomer into the interphase. The growth of the membrane is assumed to take place in the organic phase as the monomer is part of the oil phase and as it is described in existing literature on interfacial polymerization [153]. In order to help the wall formation, IPM is employed to change the solubility of the monomer or formed oligomers/polymer in the oil phase, as shown in Figure 2.3. IPM, represented with a red diamond, is fairly distant in the Hansen solubility space from to the majority of the PRMs (Figure 2.3). Hence, it reduces the solubility of the monomer and makes the monomer or formed polymer more likely to diffuse towards the interphase. Since the solubility of oligomers in the dispersed droplet phase is correlated to the rate of polymer precipitation at the interphase [9]. The role of IPM as partitioning modifier is key during radical polymerizations since by increasing the ability of the polymer to migrate to the interphase, it ensures enough monomer for the continuing the chain propagation and avoiding the chain termination [154]. As a result, high speed in the progressive in-solubilization of the polymer generally leads to denser membranes [155].

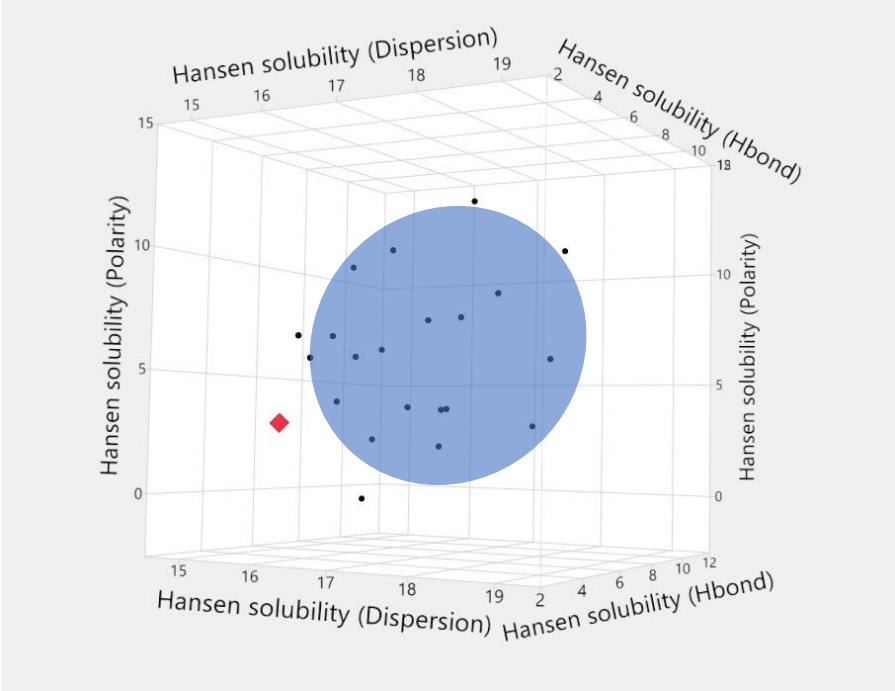

Figure 2.3 HSP of perfume raw material in the HSP space

Moreover, the Water phase contains a certain amount of polyvinyl alcohol (PVA) which is an emulsifier agent.

The temperature profile was established using the half-life in solution for each initiator at specific temperatures: 52°C for 2,2'-azobis(2,4-dimethylpentanenitrile - Vazo™ 52), 67°C for 2,-Azobis(2-methylpropionitrile - Vazo™ 67), and 70°C for 4,4′-Azobis(4-cyanovaleric acid). As it can be seen in Figure 2.4 the temperature profile contatins a constant temperature set point for each initiator half life temperature.

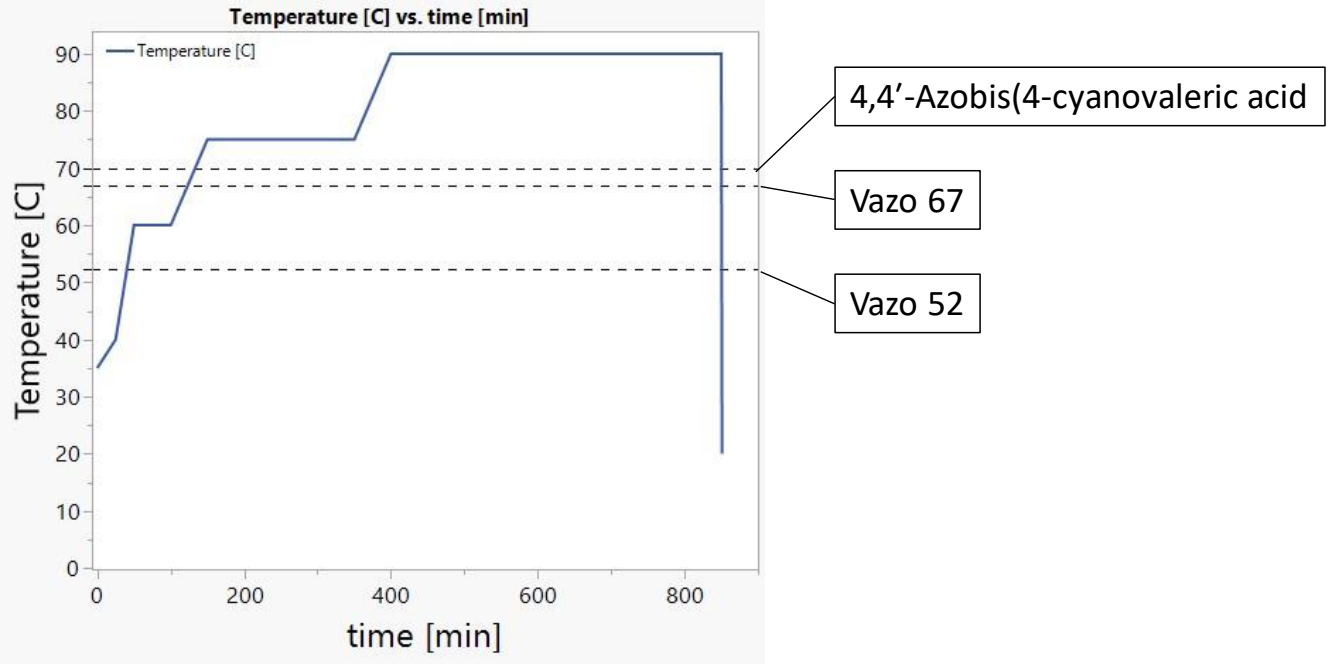

Figure 2.4: Temperature profile for the capsule synthesis

For measuring the *On-Fabric Delivery*, IEC A Base detergent was supplied from WFK Testgewebe GmbH.

LFE (Liquid Fabric Enhacer) was provided by The Procter &Gamble Company(Strombeek Bever, Belgium).

2.2.2.2 Micro-mechanical compression testing of capsules

The microcapsule slurry was diluted in 5 ml of deionized water with a dilution ratio 1:1000. Small droplets of the diluted solution were deposited on laboratory slides priorly glued on top of nanoindentation stubs with hot mounting compounds. The solvent evaporated before testing.

Nanoindentation measurements were performed using a Nanoindenter iNano (KLA Corp.) equipped with an inForce50 actuator (KLA Corp.), to measure the compressive strength of the hollow polymeric microspheres. The experimental setup utilizes the Nanoindenter actuator with a flat punch diamond tip with a diameter of 100 μm, which applies controlled compression to the microspheres until rupture occurs.

The compression process consists of two distinct phases. In the initial phase, the displacement of the punch is controlled, ensuring precise measurement and control of the applied force.

The surface identification procedure begins with the initial determination of the substrate position in an area adjacent to the microsphere of interest. Once the substrate position is identified, the system is positioned above the microsphere, and the indenter tip oscillates at the resonant frequency specific to the nanoindentation system being used. These oscillations are performed under force control, with an amplitude of approximately ±10 nm around zero position.

The compression phase is conducted without imposed oscillation, and rupture is identified through the derivative of the load signal. Rupture manifests as a sudden change in the load-depth curve. In load-controlled instruments, this sudden variation corresponds to a rapid change in displacement, while in displacement-controlled instruments, it corresponds to an immediate change in the applied load. The employed instrument implements a pseudo-displacement-controlled protocol between the two characteristics above.

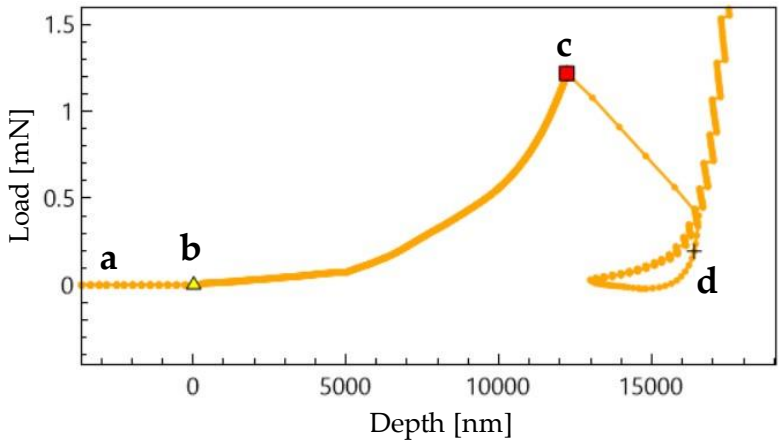

Figure 2.5: Load vs. Depth compression test of single Microcapsule.

Figure 2.5 illustrates the relationship between Load and Depth as the compression of a single Microcapsule progresses. The different point labels are linked to the time-lapse of the compression, which is presented in *Figure 2.6*. Initially, at point (a), the Nanoindenter tip approaches the microcapsule. At point (b), the tip comes into contact with the microcapsule, leading to a subsequent increase in Load as the microcapsule is compressed. At point (c), the microcapsule ruptures. Subsequently, at point (d), the tip compresses the substrate, resulting in an exponential rise in Load.

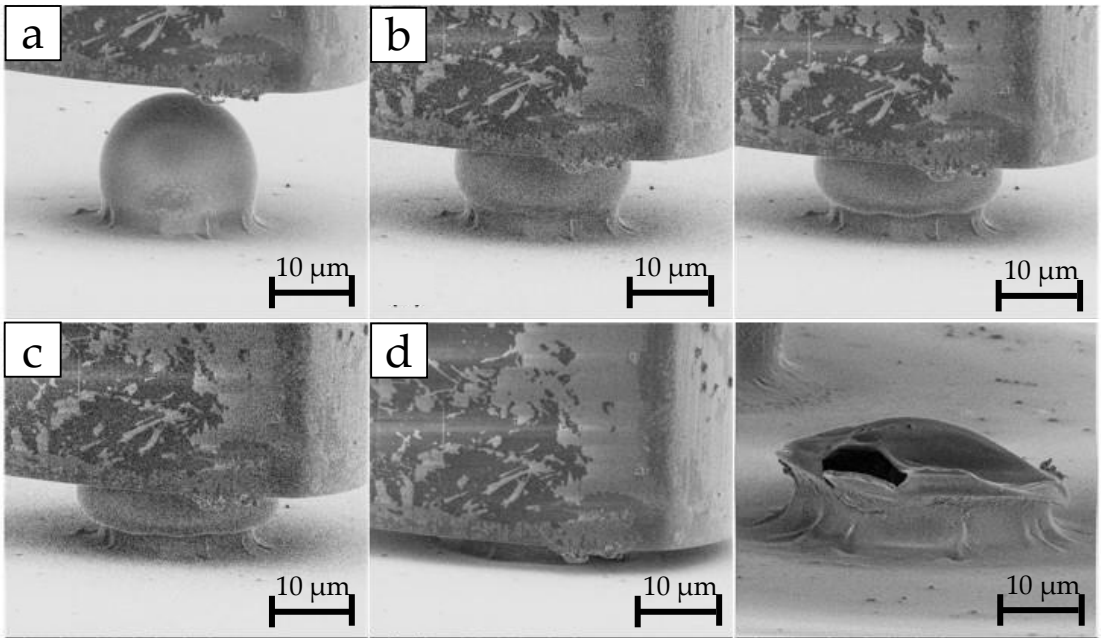

Figure 2.6: in-SITU nanoindentation time-lapse of the compression of the capsule.

The rupture force corresponds to the maximum load applied just before rupture, which in the Load vs Depth graph of *Figure 2.5* corresponds to point (c).

To determine the diameter of the microsphere, a mechanical approach is utilized. The displacement position at which the surface is identified is compared to the displacement position at which the substrate is initially detected.

Compression tests are conducted at a constant velocity of 2 μm/s in all cases. This uniform velocity ensures that any potential effects related to strain rate on the behavior of the polymeric membranes, which are sensitive to such factors, are decoupled and minimized. The compressive strength of the microspheres is ultimately determined by various factors, including the force exerted by the contents encapsulated within the microsphere, the chemistry and microstructure of the polymer membrane, and the thickness of the membrane.

2.2.2.3 Formulation into Household products

The microcapsules are formulated in a Liquid Fabric Enhancer (*LFE*) to evaluate the delivery efficiency. Microcapsules are added to the *LFE* to achieve a final perfume concentration of 0.3% through the use of microcapsules. The concentration of perfume in the microcapsules is defined as the percentage in weight

of active (perfume) to the total weight of the microcapsules slurry. The composition of the LFE is shown in Table 2.2.

Table 2.2: LFE formulation comprising microcapsules.

Ingredient	wt.%
Softening active	7.0
Formic acid	$4.5 \cdot 10^{-2}$
Sodium hydroxyethane diphosphonic acid	$7.1 \cdot 10^{-3}$
Silicone antifoam	$2.0 \cdot 10^{-3}$
Perfume via MicroCapsules	$3.0 \cdot 10^{-1}$
Water	Balance to 100%

The Softening active is a Diester quaternary ammonium compound (Ci-DEEDMAC=Ditallowoyl Ethoxy Ester Dimethyl Ammonium Chloride [MDEA based, Methyl Di-Ethanol amine based quat, available from Evonik]).

2.2.2.4 Encapsulation Efficiency determination

The percentage of *Encapsulation Efficiency* in the microcapsule slurry was determined via Gas Chromatographic Mass Spectrometric Analysis. Solid-phase microextraction (SPME) (50/30µm DVB/Carboxen/PDMS) was employed.

Following the procedure outlined in *Formulation into Household product* section, two *LFE* products were made: *Microcapsules in LFE* and *Reference Oil in LFE.*

The *Microcapsules in the LFE product* was made by adding the capsule slurry to LFE, resulting in a perfume weight fraction of 0.3%. The *Reference Oil in LFE* was prepared by substituting the microcapsules with 0.3% of the same perfume oil used for the encapsulation. This ensures that the quantity of perfume is equal in both products. Two replicates of each product (*Microcapsules in LFE* and *Reference Oil in LFE*) were injected into sealed Headspace vials and then allowed to equilibrate for 3 hours at room temperature before being analyzed by GC-MS. The GC-MS analyses were performed by sampling the headspace of each vial via SPME with a vial penetration of 25 mm and an extraction time of 1 minute at

room temperature. Ion extraction of the specific mass for each component was obtained. The SPME fiber was subsequently on-line and thermally desorbed into the GC using a ramp from 40°C (0.5 min) to 270°C (0.25 min) at 17°C/min. The perfume raw materials with a molecular weight between 35 and 300 m/z were analyzed by GC/MS in full scan mode.

The sum of all the areas under the chromatogram peaks corresponding to the perfume in *Microcapsules in LFE* and *Reference Oil in LFE* were calculated as $Area_{Microcapsules\ in\ LFE}$ and $Area_{Reference\ Oil\ in\ LFE}$, respectively.

The *Free Oil %* was then calculated by Equation (2.1):

$$Free\ Oil\ \% = \frac{Area_{Microcapsules\ in\ LFE}}{Area_{Reference\ Oil\ in\ LFE}} \cdot 100 \tag{2.1}$$

The *Free Oil %* is defined as the perfume outside the capsule core. Hence it indicates the amount of perfume that either was not successfully encapsulated or that has already leaked out in the outer slurry formulation at the time of analysis. *The Free Oil %* values are then calculated in terms of *Encapsulation Efficiency (EE %)* by Equation (2.2)

$$EE\ \% = \frac{100 - Free\ Oil\%}{100} \cdot 100 \tag{2.2}$$

2.2.2.5 GC-MS On-Fabric Delivery Assessment

The *On-Fabric Delivery* assessment was carried out via P&G standard method TMD01389. Miele w1714washing machines were used to treat the fabrics. For each treatment, the washing machine was loaded with 3kg of fabrics, comprising terry towel cotton fabric tracers and a mixed load of fabrics. The terry towel cotton fabrics weights about 870g, while the mixed load of fabrics contains about 1065g knitted cotton fabric and about 1065g polyester-cotton fabrics, to follow a ratio of 50/50 between cotton and polyester fabrics. Additionally, the fabric load comprises twenty terry towel tracers.

Before the wash, the machine was cleaned out. In total, four ethanol wipes were used: one for the first half of the inox drum; another one for the second half of the inox drum; the third wipe for the rubber of the washing machine; the fourth for the washing machine drawer. The washing machine was left open for a minimum of one minute. Then one washing cycle was run at 95°C. Moreover, before the test treatment, the load was preconditioned twice, each time using the 95°C short cotton cycle with 79g of

unperfumed IEC A Base detergent from WFK Testgewebe GmbH, followed by two additional 95°C washes without detergent.

For the test treatment, the fabric load was washed using a 30°C short cotton cycle, 1200rpm spin speed with 79g IEC A Base detergent, added at the start of the wash cycle in the appropriate dispenser. A dosage of 40 ml of the LFE fabric treatment composition described in *Table 2.2* was added to the suitable dispenser.

At the end of the wash cycle, the fabric tracers were removed from the washing machine and were line-dried overnight for around 12 hours in a closed room. Two 4x4cm fabric aliquots are cut from two terry towel cotton tracers and are transferred to 25 mL Headspace vials. The headspace above the fabric tracers was analyzed using the SPME headspace GC/MS (gas chromatography/mass spectrometry) approach described in the *Encapsulation Efficiency determination* section.

The amount of perfume in the headspace is expressed as nmol/L.

2.3 Results & Discussions

2.3.1 Capsule Characterization

The detailed composition of the batches under investigation is shown in Table 3. The monomer mixture employed is the sole parameter that differed in making the various samples. The monomer composition and weight proportions variations are introduced to establish a structure-performance correlation.

For the sake of clarity, the names of the samples are defined as follows: CAP|CN975|CM6|M8|, where CN975, CM6, M8 correspond to the weight ratio of Monomer CN975, Monomer CM6, and Monomer M8, while X is equal to the value of shell to core ratio. The shell/core ratio for all the samples equals 5:95, where the Core is defined as the weighted sum of the fragrance and IPM, while the shell is defined as the sum of acrylic monomers.

Table 2.3: Monomer composition of capsules synthesized.

Sample Name	Monomer mixture composition (wt.%)			Shell:Core ratio(wt.%)
	%CN975	%CM6	%M8	
CAP|1|0|0-5|-5	100	0	0	5:95
CAP|0|1|0|-5	0	100	0	5:95

CAP|0.3|0.7|0|-5	30	70	0	5:95
CAP|0.5|0.5|0-5	50	50	0	5:95
CAP|0|0|1|-5	0	0	100	5:95
CAP|0.3|0|0.7|-5	30	0	70	5:95
CAP|0.5|0|0.5|-5	50	0	50	5:95

To provide a quantification parameter to characterize the molecular structure of the capsule wall, the Molecular weight between cross-links (MW_c) is defined. The MW between cross-links is a parameter that characterizes the average distance between cross-linking points in the polymer network. Since acrylic monomer conversion is reported to reach practically 100% value [103, 104], it was reasonably assumed that the acrylic conversion is complete. Under this hypothesis, the molecular weight between cross-links can be calculated by dividing the average molecular weight of the monomers (M_{av}) by the number of acrylic groups per molecule (c) [105] as shown in Equation (2.3):

$$MW_c = \frac{M_{av}}{c} \tag{2.3}$$

In Table 2.4, the batches of capsules are characterized in terms of their molecular structures, such by MW_c and HSP Distance. The Volume-weighted mean diameter (VW Mean Diameter) is reported as calculated via AccuSizer 780 AD, which leverages single-particle optical sensing (SPOS) [27][28].

Table 2.4: Characterization of capsule batches in terms of MW_c and Hansen Solubility Distance

Sample Name	**Monomer mixture (wt.%)**			**MW between cross-links**	**HSP Distance**	**VW Mean Diameter [μm]**
	%CN975	**%CM6**	**%M8**			
CAP|1|0|0-5|-5	100	0	0	128	1	20
CAP|0|1|0|-5	0	100	0	172	0.46	18
CAP|0.3|0.7|0|-5	30	70	0	147	0.58	24
CAP|0.5|0.5|0-5|-5	50	50	0	139	0.69	24
CAP|0|0|1|-5	0	0	100	105	0.34	21

CAP|0.3|0|0.7|-5	30	0	70	112	0.52	22
CAP|0.5|0|0.5|-5	50	0	50	117	0.65	21

The morphology of the prepared batches was characterized by scanning electron microscopy (SEM) Hitachi FlexSEM 1000. The images for the batches of *Table 2.4* are shown in Figure 5.

When the capsules with the highest MW_c (CAP|0|1|0|-5) were included in the SEM environment, they completely collapsed, presenting a highly distorted morphology. In contrast, the other capsules with lower MW_c exhibited a more intact appearance. This visual discrepancy suggests that CAP|0|1|0|-5 is characterized by poor encapsulation quality. The reason for this poor structural integrity will be discussed in the Discussion section.

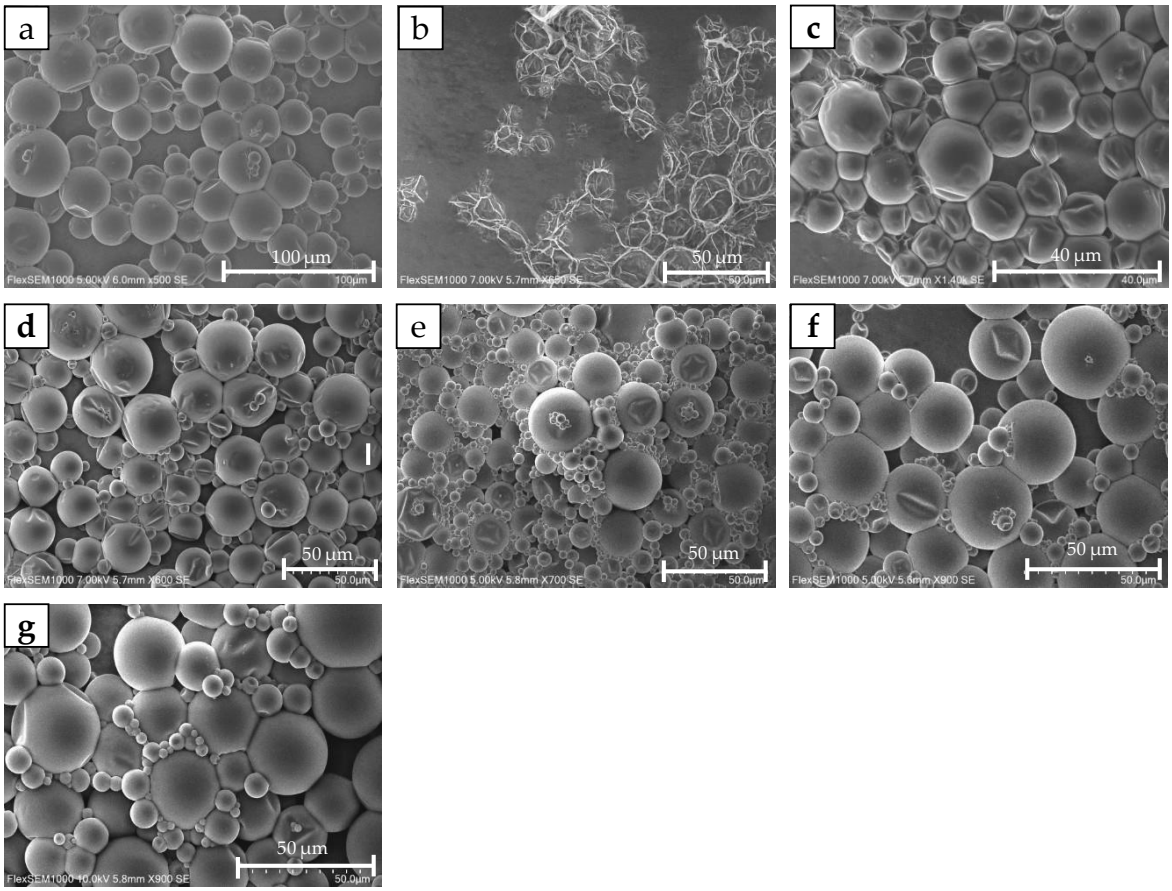

Figure 2.7: SEM micrographs of the microcapsules slurries: (a) CAP|1|0|0-5, (b) CAP|0|1|0|-5, (c) CAP|0.3|0.7|0|-5, (d) CAP|0.5|0.5|0-5|-5, (e) CAP|0|0|1|-5, (f) CAP|0.3|0|0.7|-5, (g) CAP|0.5|0|0.5|-5

The batch samples were then mechanically characterized with the abovementioned Nanoindentation protocol. The Rupture Force of the individual capsules versus their diameters was then plotted in Figure 2.8.

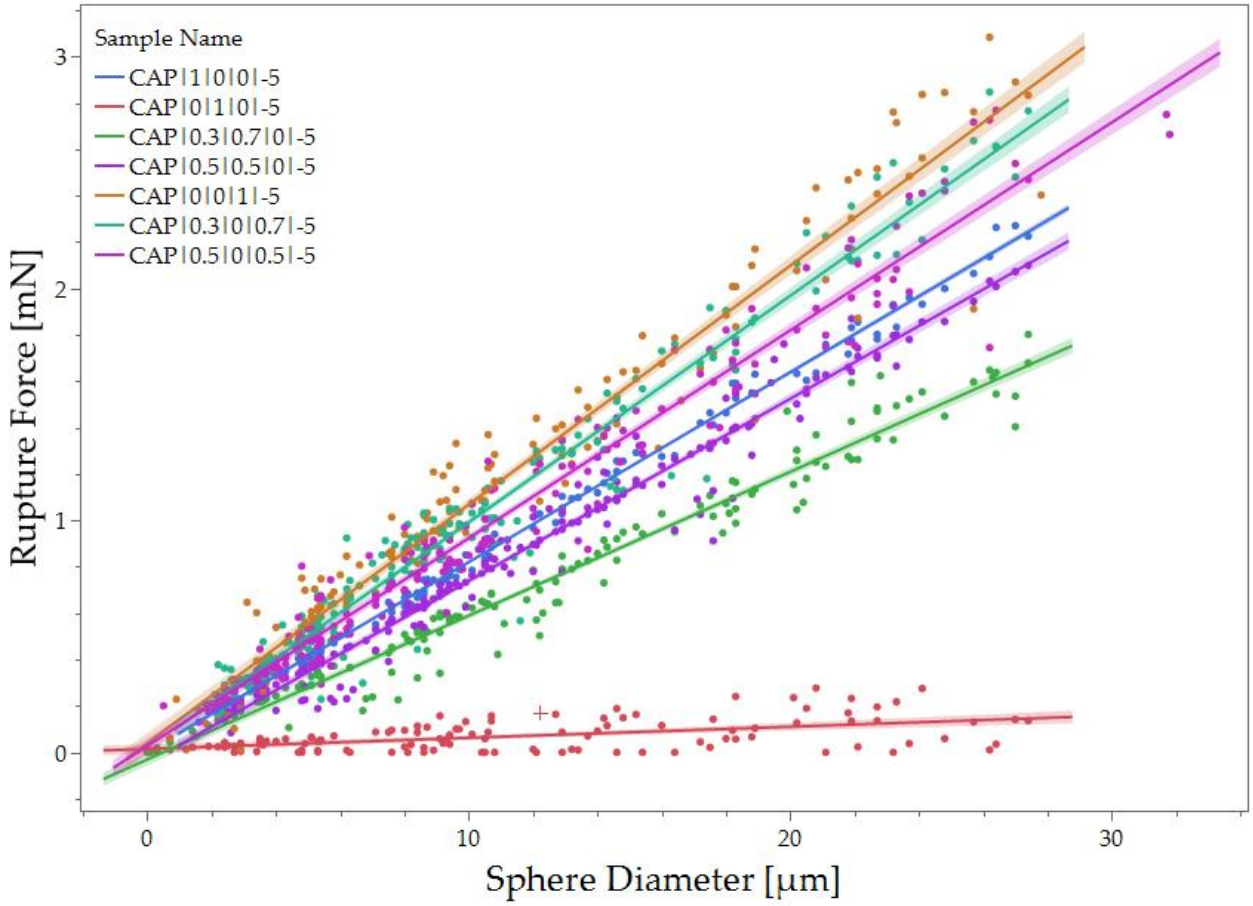

Figure 2.8: Rupture Force for each sample population plotted in function of the diameter. Linear regression and 95% confidence intervals are reported for each sample.

A linear relationship between the force required to break a capsule and its diameter can be evidenced, as highlighted in Figure 2.8. In other words, the size of the capsule has a direct impact on its mechanical properties. Larger capsules have a greater surface area and volume compared to smaller ones. This increased surface area allows for a more extensive stress distribution when external forces are applied. As a result, the load is distributed over a larger area, reducing the stress concentration on any particular point within the capsule.

Consequently, the force required to cause rupture increases in proportion to the diameter of the capsule. Furthermore, the internal volume of the capsule also influences its mechanical properties. This higher internal volume for larger capsules can contribute to the capsule's overall structural stability and strength, requiring a higher force to break the capsule.

A first-order linear regression analysis with a zero intercept was conducted to predict the value of Rupture Force as a function of the capsule diameter. As a result, the relationship between Rupture Force and diameter is highlighted by Equation (2.4):

$$Rupture\ Force = K * Diameter \tag{2.4}$$

The zero intercept was chosen to interpolate the boundary condition for an infinitely small capsule, equivalent to a capsule with a diameter of zero, which would theoretically have an infinitely small Rupture Force. In Equation 4, the variable *K* represents the linear regression slope, establishing the relationship between Rupture Force and diameter. As such, this ratio is the *average Rupture Force per unit Diameter* (*RFD*), representing the change in Rupture Force per unit diameter. The term average refers to the interpolation over the distribution of diameters, making *RFD* a material characteristic property of each tested wall composition.

RFD is believed to provide a more realistic measure of a microcapsule's ability to withstand compressive stress before rupturing, compared to Rupture Stress, as defined by Long et al. [156]. The Rupture Stress depends on specific geometric elements, such as the surface area before deformation, while *RFD* remains constant within the same capsule population, regardless of the microcapsule size. Moreover, using the Rupture Stress (given its bulk-equivalent parameter nature) might lead to incomplete interpretations:

- The stress distribution within the membrane might not be uniform [157]. Due to geometry and material properties, different membrane regions might experience different stress levels. Using simple average stress might not accurately capture this non-uniform distribution.
- Polymeric materials often have complex microstructures that can influence their mechanical behavior [158]. A bulk-based calculation might overlook microstructural effects that significantly affect fracture toughness at the micro-scale.
- At the micro-scale, the size of the membrane becomes comparable to the characteristic length scales of the material microstructure. This can lead to size-dependent mechanical behavior, such

as enhanced increased brittleness. Simply scaling down bulk properties might not account for these size effects.

In summary, using the Rupture Stress alone might oversimplify the polymeric membrane's mechanical behaviour during compression testing at the micro-scale. The *RFD* parameter, instead, is not related to the computation of the stress distribution in the membrane at incipient failure; it can provide several advantages for this specific application:

- Calculating stress distribution within a complex micro-scale membrane can be challenging. It might require advanced techniques like finite element analysis, which can be computationally intensive and require accurate material property data [159, 160, 161]. Using the rupture load is simpler, making it a practical choice when detailed stress analysis is complex.
- The *RFD* provides a conservative estimate of the material's strength. It represents the maximum load the population of micro-capsules can withstand before failing.
- Comparative Analysis: The RFD provides a direct and easy-to-understand metric when comparing different populations. It allows, indeed, to quickly assess which compositional population is stronger or more resistant to rupture.

An example illustrating the significance of *RFD* can be demonstrated through the influence of wall thickness. As the capsule consists of a core/wall structure, the wall thickness plays a crucial role in determining the overall strength of the capsule.

RFD, being a holistic material characteristic property, considers the contribution of the wall thickness to the capsule's overall strength. This allows *RFD* to effectively capture the variations in wall thickness within the population of capsules.

In summary, *RFD* comprehensively characterizes the material's behavior under the incipient loading limit relative to the diameter.

In Table 2.5 the *RFD* is reported for each sample along with the Standard Error associated with the calculation of *RFD* via the regression slope between Rupture Force and diameter.

Table 2.5: Mechanical characterization of the different Capsule batches.

Sample Name	MW between cross-links [g/mol]	RFD [mN/μm]
CAP|1|0|0-5|-5	128	$8.5 \cdot 10^{-2} \pm 6.1 \cdot 10^{-4}$
CAP|0|1|0|-5	172	$7.7 \cdot 10^{-3} \pm 5.1 \cdot 10^{-4}$
CAP|0.3|0.7|0|-5	147	$6.0 \cdot 10^{-2} \pm 4.8 \cdot 10^{-4}$
CAP|0.5|0.5|0-5|-5	139	$7.5 \cdot 10^{-2} \pm 5.2 \cdot 10^{-4}$
CAP|0|0|1|-5	105	$1.1 \cdot 10^{-1} \pm 9.7 \cdot 10^{-4}$
CAP|0.3|0|0.7|-5	112	$9.1 \cdot 10^{-2} \pm 7.4 \cdot 10^{-4}$
CAP||0.5|0|0.5|	117	$9.9 \cdot 10^{-2} \pm 7.8 \cdot 10^{-4}$

The capsule batches were analyzed for their performance regarding *Encapsulation Efficiency* and *On-Fabric Delivery*.

The results are reported in Table 2.6.

Table 2.6: Performance characterization of the capsules in terms of Encapsulation Efficiency and On-Fabric Delivery

Sample Name	Encapsulation Efficiency [%]	On-Fabric Delivery [nmol/L]
CAP|1|0|0-5|-5	94.3 ± 0.2	307.5 ± 45.7
CAP|0|1|0|-5	0	50.02 ± 12
CAP|0.3|0.7|0|-5	83.8 ± 0.3	319.6 ± 19.5
CAP|0.5|0.5|0-5|-5	89.6 ± 0.2	322.1 ± 47.9
CAP|0|0|1|-5	95.1 ± 0.3	201.3 ± 51.3
CAP|0.3|0|0.7|-5	94.8 ± 0.2	248.1 ± 49.8
CAP|0.5|0|0.5|-5	94.3 ± 0.3	260.7 ± 9.6

2.3.2 Multivariate analysis

In Figure 2.9, a Multi-variate Analysis was conducted by generating a scatterplot matrix to assess the correlation between the parameters related to the chemical structures of the monomer mixture employed (*MW_c*, *HSP distance*), and the parameters related to the performance of the capsules (*RFD*, *Encapsulation Efficiency %*, *On-Fabric Delivery*). A logarithm transformation is applied for the *Encapsulation Efficiency %* values to address the data's non-normality, as explained in the Supporting Information document.

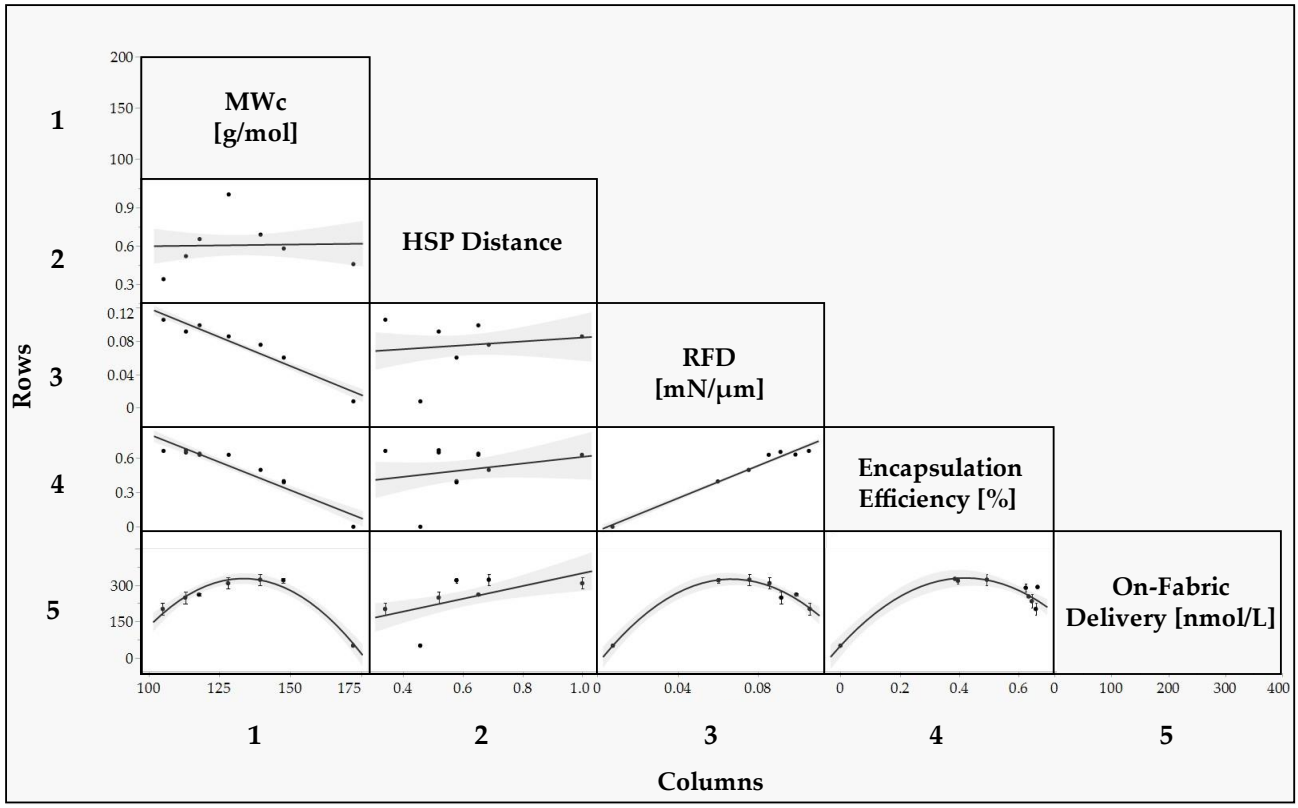

Figure 2.9: Scatter plot matrix between the chemical structure variables (MW_c, HSP Distance) and performance variables (RFD, Encapsulation Efficiency % and On-Fabric Delivery). The Structure-Performance correlations are presented as follows:

- *Row 1 and Column 1 represent the correlations comprising the molecular weight between Cross-links (MW_c)*
- *Row 2 and Column 2 represents the correlations comprising the HSP distance*
- *Row 3 and Column 3 represent the correlations comprising the RFD*

- *Row 4 and Column 4 represent the correlations comprising the Encapsulation Efficiency%*
- *Row 5 and Column 5 represent the correlations comprising On Fabric Delivery*

The relationship between MW_c and *RFD* highlights that increasing MW_c leads to a decrease in the force required to break each capsule. This correlation is supported by a R^2 value of 0.9.

Low values in MW_c indicate a higher density of cross-links within the encapsulating shell's given volume. Consequently, this tightly interconnected structure enhances the capsule resistance against external mechanical forces, resulting in a higher force required to break the capsules. Conversely, high values of MW_c indicate a more loosely interconnected wall structure, which reduces the capsule resistance to applied forces. The influence of polymer activity and cross-linking density on the elastic modulus and hardness can be significant and understood through the underlying microstructural changes that occur with these parameters. Polymer activity, often related to the glass transition temperature (Tg), affects the mobility of polymer chains. Polymer activity increases at higher temperatures or with more flexible chains, increasing segmental mobility. This leads to decreased elastic modulus and hardness since the polymer chains can more easily deform under the applied load during nanoindentation [162, 163].

On the other hand, cross-linking density has a pronounced effect on the mechanical properties of polymers. Cross-links act as physical constraints, limiting chain mobility and increasing the stiffness of the polymer network. As the cross-linking density increases, the elastic modulus and hardness of the polymer generally increase as well. This is because the network becomes more resistant to deformation, and the polymer chains are constrained in motion, resulting in a stiffer and harder material [164, 165, 166].

Overall, MW_c serves as a reliable predictor for both *RFD* and *Encapsulation Efficiency* (*EE*), highlighting their collinearity. This can be explained by the fact that higher values of *EE* indicate better quality of encapsulation and, consequently, improved mechanical strength. The collinearity between *RFD* and *EE* suggests they can be interchangeable, as demonstrated by samples like CAP|0|1|0|-5, which exhibited *EE* equal to 0 % and the lowest *RFD* value in the experimental campaign. Similarly, CAP|0.5|0.5|0-5|-5 displayed a high *EE* and the highest *RFD*. However, it is essential to note that *EE* and *RFD* cannot be substituted entirely for each other. For instance, in the range of *EE*% from 94% to 96%, the collinearity is not fully met, as CAP|0|0|1|-5, CAP|0.3|0|0.7|-5 and CAP|0.5|0.5|0-5|-5 did not significantly differ in

terms of *EE*, while there was a noticeable variation in *RFD.* This discrepancy arises due to the distinct physical meanings of these parameters, emphasizing the importance of considering *RFD* and *EE* separately.

The *HSP Distance* provides valuable information on the solubility of the monomer mixture in the perfume mixture, which is expected to be a relevant parameter in the encapsulation process since it affects the transfer of the monomer to the interphase during encapsulation. However, in this specific case, solubility does not seem to be a parameter strongly influencing the performance of these samples since the correlation between *EE* and *HSP Distance* was not statistically significant, as highlighted by a low R^2. Since all the samples, except CAP|0|1|0|-5, exhibited good morphological characteristics, according to the SEM pictures, and relatively high *EE*, it appears that for all these samples, the *HSP Distance* between the monomer mixture and the perfume mixture is enough to enable a satisfactory transfer of monomer to the interphase, hence a successful encapsulation.

Overall, the higher correlation between *RFD* and *EE* indicates that MW_c is the predominant chemical parameter in determining the encapsulation outcome, rather than the *HSP Distance*. This suggests that controlling the MW_c is crucial for achieving desired encapsulation results within the molecular structures included in this study.

To further understand the influence of monomer solubility on the capsule, it would be valuable to test monomer differences with higher differences in *HSP Distance*. Similarly, in future studies, it would be worth evaluating perfume leakage over time, as the HSP Distance can strongly influence this parameter since the more the perfume is soluble in the wall membrane, the effortlessly it would permeate through. Lastly, solubility parameters beyond the *HSP Distance*, such as solubility computed via Cosmotherm [167], should be considered for further research to broaden the understanding of monomer-perfume interactions beyond *HSP Distance.*

Interestingly, the relationship between all variables and *On-Fabric Delivery* is not linear; instead, a quadratic prediction was employed. This is due to the complex nature of the delivery of perfume microcapsules into fabrics during a wash cycle, which involves random events such as capsule deposition and retention [168]. The deposition and retention of capsules are influenced by the surface affinity between the capsule wall and the fabric, which involves steps not thoroughly investigated in this study. Hence, the correlation appears more intricate than a linear relationship.

Figure 7 highlights that the most correlated parameter with *On-Fabric Delivery* is *RFD*. This suggests that the wash cycle, involving both low-speed and high-speed rotations [169], significantly affects the mechanical integrity of the capsules and, consequently, the mechanical strength of the capsules affects the *On-Fabric Delivery*.

The scatter plot highlights a parabolic trend between *RFD* and *On-Fabric Delivery*, indicating an optimal balance between capsule strength and perfume release. An increasing relationship for *RFD* values lower than $6.0 \cdot 10^{-2}$ mN/μm is observed, while beyond the $6.0 \cdot 10^{-2}$ mN/μm threshold, the relationship changes to decreasing. Stronger capsules are believed to resist better to rupture and remain intact under the mechanical stress of the washing machine. Their increased strength enables them to withstand rigorous conditions, avoiding premature rupture and maintaining structural integrity. As a result, more capsules can be deposited onto the fabric surface without breaking, leading to a linear rise in *On-Fabric Delivery*. However, beyond the optimal balance point of $6.0 \cdot 10^{-2}$ mN/μm, further increases in rupture force may not necessarily result in a proportional increase in the number of deposited capsules. Excessive increases in capsule strength can hinder perfume release: indeed, when the capsules become excessively strong, they may be less prone to rupture even under normal usage conditions, thus limiting the release of the encapsulated perfume.

2.4 Conclusions

Understanding the influence of the chemical structure of the wall composition on mechanical properties and delivery efficiency is crucial for enhancing encapsulation efficiency.

For acrylic-based microcapsules, upon decreasing the MW_c of the monomer mixture from 175 g/mol to 100 g/mol, an improvement was observed both in terms of *RFD* (increase from 0.01 ± 5.1 $\cdot 10^{-4}$ to 0.1 ± 9.7 $\cdot 10^{-4}$ mN/μm) and in terms of *Encapsulation Efficiency* (increase from 0% to 95.1 ± 0.3%). This trend is believed to be primarily related to a higher cross-linking density which acts as a physical constraint, limiting chain mobility and increasing the stiffness of the polymer network.

In the context of this study, CAP|1|0|0-5|-5, CAP|0.3|0|0.7|-5 and CAP|0.5|0.5|0-5|-5, composed of combinations of (oligoglycolate diacrylate)ethylene glycol and CN975, achieved the highest *On-Fabric delivery* (approximately 300 nmol/L) in a Liquid Fabric Enhancers (LFE) context. Ultimately, the system with 100% CN975 was preferred due to its optimal MW_c of 128 g/mol, resulting in the ideal *On-Fabric delivery* (307.5 ± 45.7 nmol/L) driven by an *RFD* of 8.5$\cdot 10^{-2}$ ± 6.1$\cdot 10^{-4}$ mN/μm and an *Encapsulation Efficiency* of 94.3 ± 0.2 %.

By selecting the molecular structure of the capsule wall, mainly via choosing the optimal range of MW_c it becomes possible to modulate the cross-linking density and, consequently, the mechanical properties of the encapsulating shell. This modulation is essential for optimizing the delivery efficiency in each specific application.

As a result, more efficient microcapsules enable a reduction in the use of perfume and actives in the formulation, thereby providing sustainability benefits through the more efficient use of chemistry. Moreover, properly selecting acrylic monomers could also optimize other microcapsule properties, such as environmental impact and affinity to the core materials.

Bibliography

[1] G. Fanger, A Brief History and Introduction, Boston, MA: Springer, 1974.

[2] H. Y. Lee, S. J. Lee, I. W. Cheong and J. H. Kim, Microencapsulation of fragrant oil via in situ polymerization: effects of pH and melamine-formaldehyde molar ratio, vol. 19, Taylor & Francis, 2008, pp. 559-569.

[3] B. Di Credico, M. Levi and S. Turri, An efficient method for the output of new self-repairing materials through a reactive isocyanate encapsulation, vol. 49, Pergamon, 2013, pp. 2467-2476.

[4] C. E. Mora-Huertas, H. Fessi and A. Elaissari, "Polymer-based nanocapsules for drug delivery," vol. 385, no. 1-2, pp. 113-142, 1 2010.

[5] V. C. F. Mosqueira, P. Legrand, A. Gulik, O. Bourdon, R. Gref, D. Labarre and G. Barratt, "Relationship between complement activation, cellular uptake and surface physicochemical aspects of novel PEG-modified nanocapsules," vol. 22, no. 22, pp. 2967-2979, 11 2001.

[6] R. Dubey, T. Shami and K. B. Rao, "Microencapsulation Technology and Applications," *Defence Science Journal*, vol. 59, pp. 82-95, 2009.

[7] A. M. Bakry, S. Abbas, B. Ali, H. Majeed, M. Y. Abouelwafa, A. Mousa and L. Liang, "Microencapsulation of Oils: A Comprehensive Review of Benefits, Techniques, and Applications," *Comprehensive Reviews in Food Science and Food Safety*, vol. 15, no. 1, pp. 143-182, 1 2016.

[8] O. Nguon, F. Lagugné-Labarthet, F. A. Brandys, J. Li and E. R. Gillies, "Microencapsulation by in situ Polymerization of Amino Resins," *Polymer Reviews*, 2017.

[9] P. Naha, V. Kanchan, P. K. Manna and A. K. Panda, "Improved bioavailability of orally delivered insulin using Eudragit-L30D coated PLGA microparticles," *Journal of Microencapsulation*, vol. 25, no. 4, pp. 248-256, 6 2008.

[10] A. P. Esser-Kahn, S. A. Odom, N. R. Sottos, S. R. White and J. S. Moore, "Triggered release from polymer capsules," vol. 44, no. 14, pp. 5539-5553, 7 2011.

[11] G. León, N. Paret, P. Fankhauser, D. Grenno, P. Erni, L. Ouali and D. L. Berthier, Formaldehyde-free melamine microcapsules as core/shell delivery systems for encapsulation of volatile active ingredients, vol. 7, The Royal Society of Chemistry, 2017, pp. 18962-18975.

[12] Y. Yeo and K. Park, "Control of encapsulation efficiency and initial burst in polymeric microparticle systems," *Archives of Pharmacal Research*, vol. 27, no. 1, pp. 1-12, 2004.

[13] L. Nordstierna, A. A. Abdalla, M. Nordin and M. Nydén, Comparison of release

behaviour from microcapsules and microspheres, vol. 69, Elsevier, 2010, pp. 49-51.

[14] I. M. Martins, S. N. Rodrigues, M. F. Barreiro and A. E. Rodrigues, "Release of Thyme Oil from Polylactide Microcapsules," vol. 50, no. 24, pp. 13752-13761, 12 2011.

[15] E. J. Carr and G. Pontrelli, "Drug delivery from microcapsules: How can we estimate the release time?," *Mathematical Biosciences,* vol. 315, p. 108216, 9 2019.

[16] M. Andersson Trojer, Y. Li, C. Abrahamsson, A. Mohamed, J. Eastoe, K. Holmberg and M. Nydén, Charged microcapsules for controlled release of hydrophobic actives. Part I: encapsulation methodology and interfacial properties, vol. 9, The Royal Society of Chemistry, 2013, pp. 1468-1477.

[17] Y. Xia, P. F. Ribeiro and D. W. Pack, Controlled protein release from monodisperse biodegradable double-wall microspheres of controllable shell thickness, vol. 172, Elsevier, 2013, pp. 707-714.

[18] Y. Gao, D. Zhao, M. W. Chang, Z. Ahmad and J. S. Li, "Optimising the shell thickness-to-radius ratio for the fabrication of oil-encapsulated polymeric microspheres," vol. 284, pp. 963-971, 1 2016.

[19] T. Matsuda, N. Jadhav, K. B. Kashi, M. Jensen, A. Suryawanshi and V. J. Gelling, "Self-healing ability and particle size effect of encapsulated cerium nitrate into pH sensitive microcapsules," vol. 90, pp. 425-430, 1 2016.

[20] R. Arshady, "Microcapsules for food," *Journal of Microencapsulation,* vol. 10, no. 4, pp. 413-435, 1993.

[21] G. E. Visscher, J. E. Pearson, J. W. Fong, G. J. Argentieri, R. L. Robison and H. V. Maulding, Effect of particle size on the in vitro and in vivo degradation rates of poly(DL-lactide-co-glycolide) microcapsules, vol. 22, John Wiley & Sons, Ltd, 1988, pp. 733-746.

[22] K. L. Jarvis, T. J. Barnes and C. A. Prestidge, "Surface chemistry of porous silicon and implications for drug encapsulation and delivery applications," vol. 175, pp. 25-38, 7 2012.

[23] C. Wischke and S. P. Schwendeman, "Review Principles of encapsulating hydrophobic drugs in PLA/PLGA microparticles," vol. 364, pp. 298-327, 2008.

[24] J. G. Werner, S. Nawar, A. A. Solovev and D. A. Weitz, "Hydrogel Microcapsules with Dynamic pH-Responsive Properties from Methacrylic Anhydride," vol. 51, no. 15, pp. 5798-5805, 8 2018.

[25] E. M. Tavera, S. B. Kadali, H. G. Bagaria, A. W. Liu and M. S. Wong, Experimental and modeling analysis of diffusive release from single-shell microcapsules, vol. 55, John Wiley & Sons, Ltd, 2009, pp. 2950-2965.

[26] D. Pirone, V. Marturano, R. Del Pezzo, S. F. Prieto, T. Underiner, M. Giamberini and B. Tylkowski, "Molecular Design of Microcapsule Shells for Visible Light-Triggered Release," vol. 11, no. 5, p. 904, 5 2019.

[27] S.-J. Park, Y.-S. Shin and J.-R. Lee, "Preparation and Characterization of Microcapsules Containing Lemon Oil," vol. 241, pp. 502-508, 2001.

[28] C. C. Loi, G. T. Eyres and E. J. Birch, "Protein-Stabilised Emulsions," pp. 404-409, 1 2019.

[29] R. Dubey, T. Shami and K. B. Rao, "Microencapsulation Technology and Applications," *Defence Science Journal*, vol. 59, no. 1, pp. 82-95, 2009.

[30] N. K. Mohammed, C. P. Tan, Y. A. Manap, B. J. Muhialdin and A. S. M. Hussin, Spray Drying for the Encapsulation of Oils—A Review, vol. 25, Multidisciplinary Digital Publishing Institute, 2020, p. 3873.

[31] A. Gharsallaoui, G. Roudaut, O. Chambin, A. Voilley and R. Saurel, "Applications of spray-drying in microencapsulation of food ingredients: An overview," vol. 40, no. 9, pp. 1107-1121, 11 2007.

[32] N. K. Mohammed, C. P. Tan, Y. A. Manap, B. J. Muhialdin and A. S. M. Hussin, "Spray Drying for the Encapsulation of Oils—A Review," *Molecules 2020, Vol. 25, Page 3873*, vol. 25, no. 17, p. 3873, 8 2020.

[33] S. A. Hogan, B. F. McNamee, E. D. O'Riordan and M. O'Sullivan, "Emulsification and microencapsulation properties of sodium caseinate/carbohydrate blends," *International Dairy Journal*, vol. 11, no. 3, pp. 137-144, 1 2001.

[34] S. Rojas-Moreno, F. Cárdenas-Bailón, G. Osorio-Revilla, T. Gallardo-Velázquez and J. Proal-Nájera, "Effects of complex coacervation-spray drying and conventional spray drying on the quality of microencapsulated orange essential oil," vol. 12, no. 1, pp. 650-660, 3 2018.

[35] A. Soottitantawat, K. Takayama, K. Okamura, D. Muranaka, H. Yoshii, T. Furuta, M. Ohkawara and P. Linko, "Microencapsulation of l-menthol by spray drying and its release characteristics," *Innovative Food Science & Emerging Technologies*, vol. 6, no. 2, pp. 163-170, 6 2005.

[36] F. Salaün, G. Bedek, E. Devaux, D. Dupont and L. Gengembre, Microencapsulation of a cooling agent by interfacial polymerization: Influence of the parameters of encapsulation on poly(urethane–urea) microparticles characteristics, vol. 370, Elsevier, 2011, pp. 23-33.

[37] J. Yang, J. Li, X. Wang, X. Li, N. Kawazoe and G. Chen, Single mammalian cell encapsulation by in situ polymerization, vol. 4, The Royal Society of Chemistry, 2016, pp. 7662-7668.

[38] N. Devi, M. Sarmah, B. Khatun and T. K. Maji, "Encapsulation of active ingredients in polysaccharide–protein complex coacervates," vol. 239, pp. 136-145, 1 2017.

[39] A. Napiórkowska and M. Kurek, "Coacervation as a Novel Method of Microencapsulation of Essential Oils—A Review," *Molecules 2022, Vol. 27, Page 5142*, vol. 27, no. 16, p. 5142, 8 2022.

[40] K. Bruyninckx and M. Dusselier, "Sustainable Chemistry Considerations for the Encapsulation of Volatile Compounds in Laundry-Type Applications," *ACS Sustainable Chemistry and Engineering*, vol. 7, no. 9, pp. 8041-8054, 5 2019.

[41] H. Pakzad, I. Alemzadeh and A. Kazemi, "Encapsulation of Peppermint Oil with Arabic Gum-gelatin by Complex Coacervation Method," vol. 26, no. 8, pp. 807-814, 8 2013.

[42] X. L. Gu, X. Zhu, X. Z. Kong and Y. Tan, "Comparisons of simple and complex coacervations for preparation of sprayable insect sex pheromone microcapsules and

release control of the encapsulated pheromone molecule," vol. 27, no. 4, pp. 355-364, 2010.

[43] Y. P. Timilsena, T. O. Akanbi, N. Khalid, B. Adhikari and C. J. Barrow, "Complex coacervation: Principles, mechanisms and applications in microencapsulation," vol. 121, pp. 1276-1286, 1 2019.

[44] A. M. Bakry, S. Abbas, B. Ali, H. Majeed, M. Y. Abouelwafa, A. Mousa and L. Liang, "Microencapsulation of Oils: A Comprehensive Review of Benefits, Techniques, and Applications," vol. 15, no. 1, pp. 143-182, 1 2016.

[45] N. V. N. Jyothi, P. M. Prasanna, S. N. Sakarkar, K. S. Prabha, P. S. Ramaiah and G. Y. Srawan, "Microencapsulation techniques, factors influencing encapsulation efficiency," vol. 27, no. 3, pp. 187-197, 2010.

[46] R. Shaddel, J. Hesari, S. Azadmard-Damirchi, H. Hamishehkar, B. Fathi-Achachlouei and Q. Huang, "Use of gelatin and gum Arabic for encapsulation of black raspberry anthocyanins by complex coacervation," *International Journal of Biological Macromolecules,* vol. 107, pp. 1800-1810, 2 2018.

[47] C. Perignon, G. Ongmayeb, R. Neufeld, Y. Frere and D. Poncelet, "Microencapsulation by interfacial polymerisation: membrane formation and structure," vol. 32, no. 1, pp. 1-15, 2 2015.

[48] F. Zhang, J. b. Fan and S. Wang, "Interfacial Polymerization: From Chemistry to Functional Materials," vol. 59, no. 49, pp. 21840-21856, 12 2020.

[49] S. N. Rodrigues, I. Fernandes, I. M. Martins, V. G. Mata, F. Barreiro and A. E. Rodrigues, "Microencapsulation of Limonene for Textile Application," vol. 47, no. 12, pp. 4142-4147, 6 2008.

[50] D. Saihi, I. Vroman, S. Giraud and S. Bourbigot, "Microencapsulation of ammonium phosphate with a polyurethane shell. Part II. Interfacial polymerization technique," vol. 66, no. 10, pp. 1118-1125, 10 2006.

[51] M. de la Paz Miguel and C. I. Vallo, "Influence of the emulsifying system to obtain linseed oil-filled microcapsules with a robust poly (melamine-formaldehyde)-based shell," vol. 129, pp. 236-246, 4 2019.

[52] S. R. Kiran and N. K. babu, "Formulation and optimization of verapamil hydrochloride microcapsules," vol. 1, no. 1, pp. 54-58, 2011.

[53] Q. Wang, J. Gong, X. Huang, H. Yu and F. Xue, "In vitro evaluation of the activity of microencapsulated carvacrol against Escherichia coli with K88 pili," vol. 107, no. 6, pp. 1781-1788, 12 2009.

[54] H. Majeed, Y.-Y. Bian, B. Ali, A. Jamil, U. Majeed, Q. F. Khan, K. J. Iqbal, C. F. Shoemaker and Z. Fang, "Essential oil encapsulations: uses, procedures, and trends," vol. 5, no. 72, pp. 58449-58463, 7 2015.

[55] C. Gomes, R. G. Moreira and E. Castell-Perez, "Poly (DL-lactide-co-glycolide) (PLGA) Nanoparticles with Entrapped trans-Cinnamaldehyde and Eugenol for Antimicrobial Delivery Applications," vol. 76, no. 2, pp. N16-N24, 3 2011.

[56] H. Alkhatib, F. Mohamed, M. E. Akkawi, M. Alfatama, B. Chatterjee and A. A. Doolaanea, "Microencapsulation of black seed oil in alginate beads for stability and taste masking," vol. 60, p. 102030, 12 2020.

[57] F. Yu, Y. Wang, Y. Zhao, J. Chou and X. Li, "Preparation of polyurea microcapsules by interfacial polymerization of isocyanate and chitosan oligosaccharide," vol. 14, no. 13, p. 3753, 7 2021.

[58] J.-C. Côté, C. Vincent, K.-H. Son and S. H. Bok, "Érudit est un consortium interuniversitaire sans but lucratif composé de l'," vol. 82, no. 2, pp. 73-82, 2001.

[59] I. M. Martins, M. F. Barreiro, M. Coelho and A. E. Rodrigues, "Microencapsulation of essential oils with biodegradable polymeric carriers for cosmetic applications," vol. 245, pp. 191-200, 6 2014.

[60] H. Kim, M. Kim, Y. Quan, T. Moon, J. Mun, H. Cho, N. Park, W. Moon, K. Lee, H. Kim, J. Lee, H. Ryoo and H. Jung, "Novel anti-wrinkle effect of cosmeceutical product with new retinyl retinoate microsphere using biodegradable polymer," *Skin Research and Technology*, vol. 18, no. 1, pp. 70-76, 2 2012.

[61] J. O. Dihora and M. A. Brown, "Shampoo compositions with increased deposition of polyacrylate microcapsules". Patent US10143632B2, 2012.

[62] J. H. Jiten Odhavji Dihora, "Conditioner compositions with increased deposition of polyacrylate microcapsules". Patent US9561169B2, 2015.

[63] M. Goldberg and D. M. Kellner, "Antiperspirant/deodorant containing microcapsules," 12 1990.

[64] D. J. Rowe, Chemistry and Technology of Flavours and Fragrances, Wiley Blackwell, 2009, pp. 1-336.

[65] S. Gane, D. Georganakis, K. Maniati, M. Vamvakias, N. Ragoussis, E. M. Skoulakis and L. Turin, "Correction: Molecular vibration-sensing component in human olfaction (PLoS ONE)," *PLoS ONE*, vol. 8, no. 5, 5 2013.

[66] V. A. Worwood, "The fragrant mind: Aromatherapy for personality, mind, mood, and emotion," 1996.

[67] H. Lee, C. H. Choi, A. Abbaspourrad, C. Wesner, M. Caggioni, T. Zhu and D. A. Weitz, Encapsulation and Enhanced Retention of Fragrance in Polymer Microcapsules, vol. 8, American Chemical Society, 2016, pp. 4007-4013.

[68] F. Casanova and L. Santos, Encapsulation of cosmetic active ingredients for topical application – a review, vol. 33, Taylor & Francis, 2015, pp. 1-17.

[69] Michael McCoy, "Delivering value in the laundry room," vol. 96, no. 5, pp. 18-21, 1 2018.

[70] M. M. K. D. Nitamani Choudhury, "Microencapsulation: An overview on concepts, methods, properties and applications in foods," *Food Frontiers*, 2021.

[71] R. Dubey, "Microencapsulation Technology and Applications," *Defence Science Journal*, vol. 59, no. 1, pp. 82-95, 1 2009.

[72] O. A. Hakeim, F. Abdelghaffar and A. A. Haroun, UV-curable hyperbranched polyester acrylate encapsulation of phthalocyanine pigments for high performance synthetic fabrics printing, vol. 177, Elsevier, 2020, p. 108307.

[73] X. Qiu, G. Song, X. Chu, X. Li and G. Tang, Preparation, thermal properties and thermal reliabilities of microencapsulated n-octadecane with acrylic-based polymer shells for thermal energy storage, vol. 551, Elsevier, 2013, pp. 136-144.

[74] A. Carreira, R. Teixeira, A. Beirão, R. V. Vieira, M. Figueiredo and M. Gil,

"Preparation of acrylic based microcapsules using different reaction conditions for thermo-regulating textiles production," *European Polymer Journal*, 2017.

[75] J. O. Dihora, J. Smets and T. A. Schwantes, "Delivery particle". US Patent US 2011/0268802 A1, 11 May 2010.

[76] S. L. M. R. M.-C. A. M. M. Marie-Christine levy, "Fourier Transform Infrared Spectroscopic Studies of Human Serum Albumin Microcapsules Prepared by Interfacial Cross-linking with Terephthaloylchloride: Influence of Polycondensation pH on Spectra and Relation with Microcapsule Morphology and Size," 1990.

[77] V. A. M. G. D. M. R. Moghbeli, "Microencapsulation of Ethion by Interfacial Polymerization Utilizing Potassium Phthalimide-N-oxyl (PPINO) as a Promoter," *Iranian Journal of Chemical Engineering*, 2011.

[78] A. D. McNaught and A. Wilkinson, IUPAC. Compendium of Chemical Terminology, 2nd ed. (the "Gold Book"), Blackwell Scientific Publications, 1997.

[79] A. Sienkiewicz, P. Krasucka and B. Charmas, "Swelling effects in cross-linked polymers by thermogravimetry.," *J Therm Anal Calorim*, p. 85–93, 2017.

[80] J. K. Fink, "Dispersions, Emulsions, and Foams," in *Petroleum Engineer's Guide to Oil Field Chemicals and Fluids,*, Gulf Professional Publishing, 2012, pp. 663-694.

[81] S. F. Prieto, J. Smets, P. Saveyn and O. Laura, "Fabric softener composition comprising encapsulated benefit agent". United States Of America; Patent US11142723B2, 16 03 2017.

[82] G. Odian, *Principles of Polymerization* , 2004.

[83] C. Hansen, Hansen Solubility Parameters: A user's handbook, CRC Press: Boca Raton, 2007.

[84] C. Hansen, "The Three Dimensional Solubility Parameter and Solvent Diffusion Coefficient and Their Importance in Surface Coating Formulation," *Danish Technical Press*, 1967.

[85] A. Bottino, G. Capannelli, S. Munari and A. Turturro, "Solubility parameters of poly(vinylidene fluoride," *Polymer Physics*, vol. 26(4), pp. 785-79, 1988.

[86] L. Chen, T. Ci, T. Li, L. Yu and a. J. Ding, "Effects of Molecular Weight Distribution of Amphiphilic Block Copolymers on Their Solubility, Micellization, and Temperature-Induced Sol–Gel Transition in Water," *Macromolecules*, vol. 47 (17), pp. 5895-5903, 2014.

[87] C. &. K. A. Loschen, "COSMOtherm as a Valuable Tool for Cocrystal Screening and Development," 2013.

[88] A. Klamt, F. Eckert and W. Arlt, "COSMO-RS: an alternative to simulation for calculating thermodynamic properties of liquid mixtures," *Annu Rev Chem Biomol Eng*, vol. 1, pp. 101-22, 2010.

[89] "BIOVIA COSMOTHERM," Dassault Systèmes, [Online]. Available: https://www.3ds.com/products-services/biovia/products/molecular-modeling-simulation/solvation-chemistry/biovia-cosmotherm/.

[90] A. Mohapatra, "Software tools for toxicology and risk assessment," in *Information Resources in Toxicology*, 2020.

[91] C. Nantasenamat, Isarankura-Na-Ayudhya, N. Chartchalerm, P. Thanakorn and

Virapong, "A Practical Overview of Quantitative Structure-Activity Relationship," *EXCLI Journal,* vol. 8, pp. 74-88, 2009.

[92] Hall Associates Consulting, [Online]. Available: http://www.molconn.com/products.html.

[93] "Edu Soft," [Online]. Available: http://www.edusoft-lc.com/molconn/manuals/400/chaptwo.html#btesi.

[94] L. Hall and L. Kier, "Electrotopological State Indices for Atom Types: A Novel Combination of Electronic, Topological, and Valence State Information," *Journal of Chemical Information and Computer Sciences,* vol. 35 (6), pp. 1039-1045, 1995.

[95] K. Atz, C. Isert, M. N. A. Böcker and S. Gisbert, "Δ-Quantum machine-learning for medicinal chemistry," *Phys. Chem. Chem. Phys.,* vol. 24, pp. 10775-10783, 2022.

[96] R. S. Pearlman, "Molecular Structure Description. The Electrotopological State By Lemont B. Kier (Virginia Commonwealth University) and Lowell H. Hall (Eastern Nazarene College).," *Journal of the American Chemical Society,* vol. 122 (26), pp. 6340-6340, 2000 .

[97] J. Xua, "Synthesis of UV-curing waterborne polyurethane-acrylate coating and its photopolymerization kinetics using FT-IR and photo-DSC methods," 2018.

[98] Y. Park, K. H. Lim DH, Park and I. Sung, "UV- and thermal-curing behaviors of dual curable adhesives based on epoxy acrylate oligomers," *International Journal of Adhesion and Adhesives 29,* pp. 710-717, 2009.

[99] J. Xu, Y. Jiang, T. Zhang, Y. Dai, D. Yang, F. Qiu, Z. Yu and P. & Yang, "Synthesis of UV-curing waterborne polyurethane-acrylate coating and its photopolymerization kinetics using FT-IR and photo-DSC methods.," *Progress in Organic Coatings,* vol. 122, p. 10–18, 2018.

[100] A. E. Rydholm, C. N. Bowman and Kristi S. Anseth, "Degradable thiol-acrylate photopolymers: polymerization and degradation behavior of an in situ forming biomaterial," *Biomaterials,* vol. 26, no. 22, pp. 4495-4506, 2005.

[101] J. Comer and K. Tam, "Lipophilicity Profiles: Theory and Measurement," *Pharmacokinetic Optimization in Drug Research,* pp. 275-304, 2 2001.

[102] A. O. Konuray, X. Fernández-Francos, À. Serra and X. Ramis, "Sequential curing of amine-acrylate-methacrylate mixtures based on selective aza-Michael addition followed by radical photopolymerization," 2016.

[103] M. Z. Fiume, "Final Report on the Safety Assessment of Acrylates Copolymer and 33 Related Cosmetic Ingredients," *International Journal of Toxicology,* vol. 21(6), pp. 1-50, 2002.

[104] I. Capek and P. Potisk, "Microemulsion and emulsion polymerization of butyl acrylate—I. Effect of the initiator type and temperature," *European Polymer Journal,* vol. 31, no. 12, pp. 1269-1277, 12 1995.

[105] R. P. Wool, "PROPERTIES OF TRIGLYCERIDE-BASED THERMOSETS," *Bio-Based Polymers and Composites,* 2005.

[106] J. M. A. Nicholas Ballard, "Radical polymerization of acrylic monomers: An overview," *Progress in Polymer Science,* vol. 79, pp. 40-60, 2018.

[107] R. A. Hites, "Calculating the Confidence and Prediction Limits of a Rate Constant

at a Given Temperature from an Arrhenius Equation Using Excel," *Journal of Chemical Education,* vol. 94, no. 3, pp. 398-400, 3 2017.

[108] X. Yu, J. Pfaendtner and L. J. Broadbelt, "Ab Initio Study of Acrylate Polymerization Reactions: Methyl Methacrylate and Methyl Acrylate Propagation," *Journal of Physical Chemistry A,* vol. 112, no. 29, pp. 6772-6782, 7 2008.

[109] H. Aguinis and M. V. a. C. Wayant, "On reporting and interpreting statistical significance and p values in medical research," *BMJ Evid Based Med,* vol. 26(2), p. 39–42, 2021.

[110] M. W. Keller and N. R. Sottos, "Mechanical properties of microcapsules used in a self-healing polymer," *Experimental Mechanics,* vol. 46, no. 6, pp. 725-733, 2006.

[111] N. V. N. Jyothi, P. M. Prasanna, S. N. Sakarkar, K. S. Prabha, P. S. Ramaiah and G. Y. Srawan, "Microencapsulation techniques, factors influencing encapsulation efficiency," *Journal of Microencapsulation,* vol. 27, no. 3, pp. 187-197, 2010.

[112] O. I. Vinogradova, "Mechanical properties of polyelectrolyte multilayer microcapsules," *Journal of Physics Condensed Matter,* vol. 16, no. 32, pp. R1105-R1134, 8 2004.

[113] V. V. Lulevich, I. L. Radtchenko, G. B. Sukhorukov and O. I. Vinogradova, "Mechanical properties of polyelectrolyte microcapsules filled with a neutral polymer," *Macromolecules,* vol. 36, no. 8, pp. 2832-2837, 2003.

[114] D. M. Rață, A. N. Cadinoiu, L. I. Atanase, G. Calin and M. Popa, "Design and characterization of dexamethasone phosphate -loaded microcapsules obtained by a double-emulsion method," *International Journal of Pharmaceutics,* vol. 639, 2023.

[115] G. D. Porta and E. Reverchon, "Nanostructured microspheres produced by supercritical fluid extraction of emulsions," *Biotechnology and Bioengineering,* vol. 100, no. 5, pp. 1020-1033, 2008.

[116] S. Tan, S. Mettu, M. D. Biviano, M. Zhou, B. Babgi, J. White, R. R. Dagastine and M. Ashokkumar, "Ultrasonic synthesis of stable oil filled microcapsules using thiolated chitosan and their characterization by AFM and numerical simulations," *Soft Matter,* vol. 12, no. 34, pp. 7212-7222, 2016.

[117] C. Yin, S. M. Chia, C. H. Quek, H. Yu, R. X. Zhuo, K. W. Leong and H. Q. Mao, "Microcapsules with improved mechanical stability for hepatocyte culture," *Biomaterials,* vol. 24, no. 10, pp. 1771-1780, 2003.

[118] M. M. Caruso, B. J. Blaiszik, H. Jin, S. R. Schelkopf, D. S. Stradley, N. R. Sottos, S. R. White and J. S. Moore, "Robust, double-walled microcapsules for self-healing polymeric materials," *ACS Applied Materials and Interfaces,* vol. 2, no. 4, pp. 1195-1199, 2010.

[119] A. Gray, S. Egan, S. Bakalis and Z. Zhang, "Determination of microcapsule physicochemical, structural, and mechanical properties," *Particuology,* vol. Volume 24, pp. 32-43, 2016.

[120] H. J. Butt, B. Cappella and M. Kappl, "Force measurements with the atomic force microscope: Technique, interpretation and applications," *Surface Science Reports,* vol. 59, no. 1-6, pp. 1-152, 10 2005.

[121] R. Mercadé-Prieto, R. Allen, Z. Zhang, D. York, J. A. Preece and T. E. Goodwin,

"Failure of elastic-plastic core–shell microcapsules under compression," *AIChE Journal*, vol. 58, no. 9, pp. 2674-2681, 9 2012.

[122] R. Mercadé-Prieto, R. Allen, D. York, J. A. Preece, T. E. Goodwin and Z. Zhang, "Determination of the Failure Stresses for Fluid-filled Microcapsules that Rupture Near the Elastic Regime," *Experimental Mechanics*, vol. 52, no. 9, pp. 1435-1445, 11 2012.

[123] R. Mercadé-Prieto, B. Nguyen, R. Allen, D. York, J. A. Preece, T. E. Goodwin and Z. Zhang, "Determination of the elastic properties of single microcapsules using micromanipulation and finite element modeling," *Chemical Engineering Science*, vol. 66, no. 10, pp. 2042-2049, 5 2011.

[124] F. Pal, D. M, S. AG, H. Mohwald and A. Fery, "Quantification of release from microcapsules upon mechanical deformation with AFM," *Soft Matter*, vol. 6, pp. 1879-83, 2010.

[125] S. Jun-Feng, X.-Y. Wang and H. Dong, "Micromechanical properties of melamine–formaldehyde microcapsules by nanoindentation: Effect of size and shell thickness," *Materials Letters*, vol. Volume 89, pp. 1-4, 2012.

[126] J. Kolker, L. Fischer, A. M. Menzel and H. Löwen, "Elastic Deformations of Spherical Core-Shell Systems Under an Equatorial Load," *Journal of Elasticity*, vol. 150, no. 1, pp. 77-89, 7 2022.

[127] S. A. Hayes, A. A. Goruppa and F. R. Jones, "Dynamic nanoindentation as a tool for the examination of polymeric materials," *Journal of Materials Research*, vol. 19, no. 11, pp. 3298-3306, 11 2004.

[128] R. F. Gibson, "A review of recent research on nanoindentation of polymer composites and their constituents," *Composites Science and Technology*, vol. 105, pp. 51-65, 12 2014.

[129] S. F. Ng, J. J. Rouse, F. D. Sanderson, V. Meidan and G. M. Eccleston, "Validation of a static Franz diffusion cell system for in vitro permeation studies," *AAPS PharmSciTech*, vol. 11, no. 3, pp. 1432-1441, 9 2010.

[130] A. E. Rodrigues, I. Nogueira and R. P. Faria, "Perfume and Flavor Engineering: A Chemical Engineering Perspective," *Molecules 2021, Vol. 26, Page 3095*, vol. 26, no. 11, p. 3095, 5 2021.

[131] D. S. Kim, B. Park, Ho, Rhim, J. Won, Lee and Y. Moo, "Preparation and characterization of crosslinked PVA/SiO 2 hybrid membranes containing sulfonic acid groups for direct methanol fuel cell applications," *Journal of Membrane Science*, vol. 240, pp. 37-48, 2004.

[132] E. Broitman, Indentation Hardness Measurements at Macro-, Micro-, and Nanoscale: A Critical Overview, Tribology Letters. 65: 23., 2017.

[133] X. Li and B. Bhushan, "A review of nanoindentation continuous stiffness measurement technique and its applications," *Materials Characterization*, vol. 48, no. 1, pp. 11-36, 2 2002.

[134] M. VanLandingham, J. S. Villarrubia, W. F. Guthrie and G. F. Meyers, "Nanoindentation of Polymers: An Overview," *Macromolecular symposia*, pp. 15-44, 2001.

[135] Nanomechanics , iNano Indentation System Operating Instructions.

[136] J. S. Wilson, Sensor Technology Handbook, Newnes, 2005.

[137] [Online]. Available: http://www.beikimco.com/. [Accessed 1 03 2019].

[138] R. Puers, "Capacitive sensors: When and how to use them," *Sensors and Actuators A: Physical*, vol. 37–38, pp. 93-105, 1993.

[139] E. Avallone, T. Baumeister and A. Sadegh, Marks' Standard Handbook for Mechanical Engineers (11th ed.), New York: McGraw-Hill, 2007.

[140] Zaber Technologies Inc., 2019. [Online]. Available: https://www.zaber.com/.

[141] B. B. Xiaodong Li, "A review of nanoindentation continuous stiffness," *Materials Characterization*, vol. 48, 2002.

[142] W. Oliver and G. Pharr, "An improved technique for determining hardness and elastic modulus using load and displacement sensing indentation experiments," *Journal of Materials Research*, vol. 7, no. 6, pp. 1564-1583, 6 1992.

[143] W. C. Oliver and G. M. Pharr, "An improved technique for determining hardness and elastic modulus using load and displacement sensing indentation experiments," 1992.

[144] E. G. Herbert and W. C. O. Pharr, "Nanoindentation and the dynamic characterization of viscoelastic solids," *Journal of Physics: applied physics*, 2008.

[145] J. Hay, P. Agee and a. E. Herbert, "Continuous stiffness measurement during instrumented indentation testing," 2010.

[146] D. Tabor, The Hardness of Metals, 2000.

[147] S. IN, "The Reissner-Sagoci problem," *Proceedings of the Glasgow Mathematical Association*, vol. 3, pp. 136-144, 1966.

[148] T. Chudoba and N. M. Jennett, "Higher accuracy analysis of instrumented indentation data obtained with pointed indenters," *Journal of Physics D: Applied Physics*, vol. 41, no. 21, 11 2008.

[149] R. Long, "Liquid permeation through plastic films," *Industrial & Engineering Chemistry Fundamentals*, vol. 4, pp. 445-451, 1965.

[150] J.-F. Su, X.-Y. Wang and H. Dong, "Micromechanical properties of melamine–formaldehyde microcapsules by nanoindentation: Effect of size and shell thickness," *Materials Letters*, vol. 89, pp. 1-4, 2014.

[151] A. Ghaemi, A. Philipp, A. Bauer, K. Last, A. Fery and S. Gekle, "Mechanical behaviour of micro-capsules and their rupture under compression," *Chemical Engineering Science*, vol. 142, pp. 236-243, 3 2016.

[152] M. Al-Nasassrah, F. Podczeck and J. Newton, "The effect of an increase in chain length on the mechanical properties of polyethylene glycols.," *Eur J Pharm Biopharm.*, Vols. 31-8, p. 46(1), 1998.

[153] G. O. R. N. Y. F. a. D. P. Carole Perignon, "Microencapsulation by interfacial polymerisation: membrane formation and structure," *Journal of Microencapsulation*, 2014.

[154] A. A. Cockram, T. J. Neal, M. J. Derry, O. O. Mykhaylyk, N. S. J. Williams, M. W. Murray, S. N. Emmett and a. S. P. Armes, "Effect of Monomer Solubility on the

Evolution of Copolymer Morphology during Polymerization-Induced Self-Assembly in Aqueous Solution," *Macromolecules*, vol. 50 (3), pp. 796-802, 2017.

[155] J. Wijmans, J. Kant, M. Mulder and C. Smolders, "Phase separation phenomena in solutions of polysulfone in mixtures of a solvent and a non solvent: Relationship with membrane formation.," *Polymer*, vol. 26, 1985.

[156] Y. Long, D. York, Z. Zhang and J. A. Preece, "Microcapsules with low content of formaldehyde: preparation and characterization," *Journal of Materials Chemistry*, vol. 19, no. 37, pp. 6882-6887, 9 2009.

[157] J. Zhang, A. Oueslati, W. Q. Shen and G. de Saxcé, "Exact elastic solution of the axisymmetric and deviatoric loaded hollow sphere," *International Journal of Pressure Vessels and Piping*, vol. 162, no. February, pp. 40-45, 2018.

[158] M. Ulbricht, "Advanced functional polymer membranes," *Polymer*, vol. 47, no. 7, pp. 2217-2262, 3 2006.

[159] Y. Sun, G. Peng, G. Dou, Y. Hu, P. Chen and T. Zhang, "A nano-compression model to characterize the elastic properties of core–shell structured microspheres," *Thin-Walled Structures*, vol. 173, no. November 2021, p. 108951, 2022.

[160] Y. Sun, G. Peng, Y. Hu, G. Dou, P. Chen and T. Zhang, "Spherical indentation model for evaluating the elastic properties of the shell of microsphere with core-shell structure," *International Journal of Solids and Structures*, Vols. 230-231, p. 111159, 2021.

[161] X. Chen, C. Li and X. X. Wei, "Stress analysis of a hollow sphere compressed between two flat platens," *International Journal of Mechanical Sciences*, vol. 118, pp. 67-76, 2016.

[162] B. D. Beake, G. A. Bell, W. Brostow and W. Chonkaew, "Nanoindentation creep and glass transition temperatures in polymers," *Polymer International*, vol. 56, no. 6, pp. 773-778, 6 2007.

[163] G. M. Odegard, T. S. Gates and H. M. Herring, "Characterization of viscoelastic properties of polymeric materials through nanoindentation," *Experimental Mechanics 2005 45:2*, vol. 45, no. 2, pp. 130-136, 4 2005.

[164] J. K. Deuschle, E. J. De Souza, E. Arzt and S. Enders, "Nanoindentation studies on crosslinking and curing effects of PDMS," *International Journal of Materials Research*, vol. 101, no. 8, pp. 1014-1023, 8 2010.

[165] G. Yiapanis, D. J. Henry, E. Evans and I. Yarovsky, "Simulations of nanoindentation of polymer surfaces: Effects of surface cross-linking on adhesion and hardness," *Journal of Physical Chemistry C*, vol. 114, no. 1, pp. 478-486, 1 2010.

[166] M. Ovsik, D. Manas, M. Manas, M. Stanek and M. Reznicek, "The Effect of Cross-Linking on Nano-Mechanical Properties of Polyamide," *Key Engineering Materials*, vol. 699, pp. 37-42, 2016.

[167] N. Hyttinen and N. L. Prisle, "Improving Solubility and Activity Estimates of Multifunctional Atmospheric Organics by Selecting Conformers in COSMO therm," *Journal of Physical Chemistry A*, vol. 124, no. 23, pp. 4801-4812, 6 2020.

[168] M. S. Manga, T. Adetomiwa, S. Marks, J. Gardy, R. S. Blackburn, S. J. Russell and D. W. York, "Deposition and retention of differently shaped micro-particles on

textiles during laundry processing," *Powder Technology*, vol. 398, p. 117143, 1 2022.

[169] S. Zaman, X. Tao, C. Cochrane and a. V. Koncar, "E-Textile Systems Reliability Assessment—A Miniaturized Accelerometer Used to Investigate Damage during Their Washing," *Sensors 21*, p. 605, 2021.

[170] D. Newey, M. A. Wilkins and H. M. Pollock, "An ultra-low-load penetration hardness tester," *Journal of physics E: Scientific instruments.*, vol. 15, pp. 119-122, 1982.

[171] K. Zhao, J. He, A. Mayer and Z. Zhang, "Effect of hydrogen on the collective behavior of dislocations in the case of nanoindentation," *Acta Materialia.*, p. 148, 2018.

[172] A. C. Fisher-Cripps, Nanoindentation, Springer, 2004.

[173] G. M. Pharr, "Measurement of mechanical properties by ultra-low load indentation," *Materials Science and Engineering*, vol. 253, pp. 151-159, 1998.

[174] W. C. Oliver and G. M. Pharr, "Measurement of hardness and elastic modulus by instrumental indentation: Advances in understanding and refinements to methodology," *Journal of materials research*, vol. 19, pp. 3-20, 2004.

[175] N. A. P. Nathan R. Richbourg, "The swollen polymer network hypothesis: Quantitativemodels of hydrogel swelling, stiffness, and solute transport," *Progress in Polymer Science* , 2020.

[176] M. Mucha, "Rheological characteristics of semi-dilute chitosan solutions," in *Macromol. Chem. Phys.*, 1997, p. 471–484.

[177] E. S. a. K. Winnicka, "Stability of Chitosan—A Challenge for Pharmaceutical and Biomedical Applications," *marine drugs*, 2015.

[178] E. Arunan, G. R. Desiraju, R. A. Klein, J. Sadlej, S. Scheiner, I. Alkorta, D. C. Clary, R. H. Crabtree and J. J. Dannenberg, " Definition of the hydrogen bond (IUPAC Recommendations 2011)," in *Pure and Applied Chemistry*, 2011, p. 1637–1641.

[179] C. S. Caraculacu AA, "Isocyanates in polyaddition processes. Structure and reactions mechanisms.," *Prog Polym Sci*, vol. 26, p. 799–851, 2001.

[180] R. D. Zhang Y, "Characterisation and applications of microcapsules obtained by interfacial polycondensation," *Journal of Microencapsulation*, vol. 29, p. 636–49., 2012.

[181] R. Smith, Biodegradable Polymers for Industrial Applications, 2005.

[182] ECHA, "Guidance for monomers and polymers," Version 3.0, 2023.

[183] European Chemical Agency (ECHA), [Online]. Available: https://echa.europa.eu/hot-topics/microplastics.

[184] "Is it safe to use cosmetics containing silica in nanoform?," [Online]. Available: https://ec.europa.eu/health/scientific_committees/docs/citizens_nanosilica_en.pdf.

[185] "OECD guideline for testing of chemicals," 1992.

[186] Scopus, "Data from "Scopus" bibliographic database accessed in October 2018 using the term "microplastic"".

[187] M. Alexander, Biodegradation and Bioremediation, 299-312: Academic Press,

2000.

[188] N. Karak, "Vegetable Oil-Based Polymers," in *Vegetable Oil-Based Polymers*, 2012, pp. 31-53.

[189] M. L. a. K. Min, "A Comparative Study of the Performance for Predicting Biodegradability Classification: The Quantitative Structure–Activity Relationship Model vs the Graph Convolutional Network," *American Chemical Society,* vol. 7, no. 4, p. 3649–3655, 2022.

[190] "http://oasis-lmc.org/products/models/environmental-fate-and-ecotoxicity/catabol-301b.aspx," OASIS. [Online].

[191] Helmholtz Association, Germany , [Online]. Available: www.ochem.eu.

[192] US EPA, [Online]. Available: https://www.epa.gov/tsca-screening-tools/epi-suitetm-estimation-program-interface.

[193] A. E. Rydholm, C. N. Bowman and K. S. Anseth, "Degradable thiol-acrylate photopolymers: polymerization and degradation behavior of an in situ forming biomaterial," *Biomaterials,* vol. 26, no. 22, pp. 4495-4506, 8 2005.

[194] J. Nicolas, B. Charleux, O. Guerret and S. Magnet, "Nitroxide-Mediated Controlled Free-Radical Emulsion Polymerization of Styrene and n-Butyl Acrylate with a Water-Soluble Alkoxyamine as Initiator," *Angewandte Chemie International Edition,* vol. 43, no. 45, pp. 6186-6189, 11 2004.

[195] T. Allen, Particle size measurement, Chapman and Hall, 1981, p. 678.

[196] S. Gouin, "Microencapsulation: industrial appraisal of existing technologies and trends," *Trends in Food Science & Technology,* vol. 15, no. 7-8, pp. 330-347, 7 2004.

[197] A. Murua, A. Portero, G. Orive, R. M. Hernández, M. de Castro and J. L. Pedraz, "Cell microencapsulation technology: Towards clinical application," *Journal of Controlled Release,* vol. 132, no. 2, pp. 76-83, 12 2008.

[198] Q. Zhang, P. P. Zhang and Q. Z. Jiao, Synthesis and Characterization of Microcapsules with Chlorpyrifos Cores and Polyurea Walls, vol. 22, No longer published by Elsevier, 2006, pp. 379-382.

[199] I. Aranaz, A. R. Alcántara, M. C. Civera, C. Arias, B. Elorza, A. H. Caballero, N. Acosta, H. Velasco, D. Mecerreyes, R. Antonio, B. Gimeno, A. María Díez-Pascual, V. C. Moreno and A. Serra, Chitosan: An Overview of Its Properties and Applications, vol. 13, Multidisciplinary Digital Publishing Institute, 2021, p. 3256.

[200] T. Kean and M. Thanou, Biodegradation, biodistribution and toxicity of chitosan, vol. 62, 2009, pp. 3-11.

[201] I. Gaytán, M. Burelo and H. Loza-Tavera, Current status on the biodegradability of acrylic polymers: microorganisms, enzymes and metabolic pathways involved, vol. 105, Appl Microbiol Biotechnol, 2021, p. 991–1006.

[202] I. Aranaz, A. R. Alcántara, M. C. Civera, C. Arias, B. Elorza, A. H. Caballero, N. Acosta, H. Velasco, D. Mecerreyes, R. Antonio, B. Gimeno, A. María Díez-Pascual, V. C. Moreno and A. Serra, Chitosan: An Overview of Its Properties and Applications, vol. 13, Multidisciplinary Digital Publishing Institute, 2021, p. 3256.

[203] K. Aiedeh, E. Gianasi, I. Orienti and V. Zecchi, Chitosan microcapsules as controlled release systems for insulin, vol. 14, Taylor & Francis, 1997, pp. 567-576.

[204] X. T. Mu, X. J. Ju, L. Zhang, X. B. Huang, Y. Faraj, Z. Liu, W. Wang, R. Xie, Y. Deng and L. Y. Chu, Chitosan microcapsule membranes with nanoscale thickness for controlled release of drugs, vol. 590, Elsevier, 2019, p. 117275.

[205] Z. Yang, Z. Zeng, Z. Xiao and H. Ji, Preparation and controllable release of chitosan/vanillin microcapsules and their application to cotton fabric, vol. 29, John Wiley & Sons, Ltd, 2014, pp. 114-120.

[206] M. D. Ibáñez, N. M. Sanchez-Ballester and M. A. Blázquez, Encapsulated Limonene: A Pleasant Lemon-Like Aroma with Promising Application in the Agri-Food Industry. A Review, vol. 25, Multidisciplinary Digital Publishing Institute, 2020, p. 2598.

[207] Y. Li, L. Ai, W. Yokoyama, C. F. Shoemaker, D. Wei, J. Ma and F. Zhong, Properties of chitosan-microencapsulated orange oil prepared by spray-drying and its stability to detergents, vol. 61, American Chemical Society, 2013, pp. 3311-3319.

[208] Y. C. Danarto and S. Distantina, Optimizing deacetylation process for chitosan production from green mussel (perna viridis) shell, vol. 1710, American Institute of Physics Inc., 2016, p. 30028.

[209] T. Ahmad Khan, K. Khiang Peh and H. Seng Ch, Reporting degree of deacetylation values of chitosan: the influence of analytical methods, vol. 5, 2002, pp. 205-212.

[210] M. Kołodziejska, K. Jankowska, M. Klak and M. Wszoła, Chitosan as an Underrated Polymer in Modern Tissue Engineering, vol. 11, Multidisciplinary Digital Publishing Institute, 2021, p. 3019.

[211] M. Mahmoudzadeh, A. Fassihi, J. Emami, N. M. Davies and F. Dorkoosh, Physicochemical, pharmaceutical and biological approaches toward designing optimized and efficient hydrophobically modified chitosan-based polymeric micelles as a nanocarrier system for targeted delivery of anticancer drugs, 2013.

[212] T. Ahmad Khan, K. Khiang Peh and H. Seng Ch, Reporting degree of deacetylation values of chitosan: the influence of analytical methods, vol. 5, 2002, pp. 205-212.

[213] N. T. Nguyen, D. Q. Hoang, N. D. Nguyen, Q. H. Nguyen and D. H. Nguyen, Preparation, characterization, and antioxidant activity of water-soluble oligochitosan, vol. 6, Walter de Gruyter GmbH, 2017, pp. 461-468.

[214] Y. C. Danarto and S. Distantina, Optimizing deacetylation process for chitosan production from green mussel (perna viridis) shell, vol. 1710, American Institute of Physics Inc., 2016, p. 30028.

[215] H. Hamedi, S. Moradi, S. M. Hudson, A. E. Tonelli and M. W. King, Chitosan based bioadhesives for biomedical applications: A review, vol. 282, Elsevier, 2022, p. 119100.

[216] C. Qin, Y. Du, L. Zong, F. Zeng, Y. Liu and B. Zhou, Effect of hemicellulase on the molecular weight and structure of chitosan, vol. 80, Elsevier, 2003, pp. 435-441.

[217] J. M. Viljoen, J. H. Steenekamp, A. F. Marais and A. F. Kotzé, Effect of moisture content, temperature and exposure time on the physical stability of chitosan powder and tablets, vol. 40, Taylor & Francis, 2014, pp. 730-742.

[218] C. Madeleine-Perdrillat, T. Karbowiak, F. Debeaufort, L. Delmotte, C. Vaulot and D. Champion, Effect of hydration on molecular dynamics and structure in chitosan films, vol. 61, Elsevier, 2016, pp. 57-65.

[219] M. Kurek, A. Guinault, A. Voilley, K. Galić and F. Debeaufort, Effect of relative humidity on carvacrol release and permeation properties of chitosan based films and coatings, vol. 144, Elsevier, 2014, pp. 9-17.

[220] G. Knupp, P. Kusch and M. Neugebauer, Identification of Flavor Components in Perfumes by Headspace Solid-Phase Microextraction and Gas Chromatography-Mass Spectrometry, vol. 79, Division of Chemical Education, 2002, p. 98.

[221] F. Yu, Y. Wang, Y. Zhao, J. Chou and X. Li, Preparation of polyurea microcapsules by interfacial polymerization of isocyanate and chitosan oligosaccharide, vol. 14, MDPI AG, 2021, p. 3753.

[222] S. Kalpakjian, Manufacturing processes for engineering materials, Addison-Wesley, 1984, p. 839.

[223] S.-C. Hsu, T.-M. Don and W.-Y. Chiu, Free radical degradation of chitosan with potassium persulfate.

[224] H. L. Ewalds and R. J. H. Wanhill, Fracture mechanics, E. Arnold, 1985, p. 304.

[225] V. C. F. Mosqueira, P. Legrand, A. Gulik, O. Bourdon, R. Gref, D. Labarre and G. Barratt, "Relationship between complement activation, cellular uptake and surface physicochemical aspects of novel PEG-modified nanocapsules," vol. 22, no. 22, pp. 2967-2979, 11 2001.

[226] C. Rojas, P. R. Duchowicz, P. Tripaldi and R. Pis Diez, "Quantitative structure–property relationship analysis for the retention index of fragrance-like compounds on a polar stationary phase," vol. 1422, pp. 277-288, 11 2015.

[227] H. Y. Lee, S. J. Lee, I. W. Cheong and J. H. Kim, "Microencapsulation of fragrant oil via in situ polymerization: effects of pH and melamine-formaldehyde molar ratio," vol. 19, no. 5, pp. 559-569, 9 2002.

[228] A. Gharsallaoui, G. Roudaut, O. Chambin, A. Voilley and R. Saurel, "Applications of spray-drying in microencapsulation of food ingredients: An overview," vol. 40, no. 9, pp. 1107-1121, 11 2007.

[229] R. Dris, J. Gasperi, V. Rocher, M. Saad, N. Renault, B. Tassin, a. Microplastic, C. Johnny Gasperi, A. Vincent Rocher, B. Mohamed Saad, A. A. Nicolas Renault and B. A. Tassin, "Microplastic contamination in an urban area: a case study in Greater Paris," 2015.

[230] A. M. Bakry, S. Abbas, B. Ali, H. Majeed, M. Y. Abouelwafa, A. Mousa and L. Liang, "Microencapsulation of Oils: A Comprehensive Review of Benefits, Techniques, and Applications," vol. 15, no. 1, pp. 143-182, 1 2016.

[231] F. Zhang, J. b. Fan and S. Wang, "Interfacial Polymerization: From Chemistry to Functional Materials," *Angewandte Chemie International Edition*, vol. 59, no. 49, pp. 21840-21856, 12 2020.

[232] S. Vorberg and I. V. Tetko, "Modeling the Biodegradability of Chemical Compounds Using the Online CHEmical Modeling Environment (OCHEM)," *Molecular Informatics*, vol. 33, no. 1, pp. 73-85, 1 2014.

[233] S. Vorberg and I. V. Tetko, "Modeling the biodegradability of chemical compounds using the online chemical modeling environment (OCHEM)," *Molecular Informatics*, vol. 33, no. 1, pp. 73-85, 2014.

[234] Y. Tokiwa and B. P. Calabia, "Biodegradability and biodegradation of poly(lactide)," *Applied Microbiology and Biotechnology*, vol. 72, no. 2, pp. 244-251, 9 2006.

[235] T. Takayama, Y. Daigaku, H. Ito and H. Takamori, "Mechanical properties of bio-absorbable PLA/PGA fiber-reinforced composites," *Journal of Mechanical Science and Technology*, vol. 28, no. 10, pp. 4151-4154, 10 2014.

[236] P. K. Samantaray, A. Little, D. M. Haddleton, T. McNally, B. Tan, Z. Sun, W. Huang, Y. Ji and C. Wan, "Poly(glycolic acid) (PGA): A versatile building block expanding high performance and sustainable bioplastic applications," *Green Chemistry*, vol. 22, no. 13, pp. 4055-4081, 7 2020.

[237] P. K. Samantaray, A. Little, D. M. Haddleton, T. McNally, B. Tan, Z. Sun, W. Huang, Y. Ji and C. Wan, "Poly(glycolic acid) (PGA): a versatile building block expanding high performance and sustainable bioplastic applications," *Green Chemistry*, vol. 22, no. 13, pp. 4055-4081, 7 2020.

[238] K. Madhavan Nampoothiri, N. R. Nair and R. P. John, "An overview of the recent developments in polylactide (PLA) research," *Bioresource Technology*, vol. 101, no. 22, pp. 8493-8501, 11 2010.

[239] Z. Ma, N. Zhao and C. Xiong, "Degradation and miscibility of poly(DL-lactic acid)/poly(glycolic acid) composite films: Effect of poly(DL-lactic-co-glycolic acid)," *Bulletin of Materials Science*, vol. 35, no. 4, pp. 575-578, 8 2012.

[240] H. Loonen, F. Lindgren, B. Hansen, W. Karcher, J. Niemelä, K. Hiromatsu, M. Takatsuki, W. Peijnenburg, E. Rorije and J. Struijś, "Prediction of biodegradability from chemical structure: Modeling of ready biodegradation test data," *Environmental Toxicology and Chemistry*, vol. 18, no. 8, pp. 1763-1768, 8 1999.

[241] A. Lombardo, F. Pizzo, E. Benfenati, A. Manganaro, T. Ferrari and G. Gini, "A new in silico classification model for ready biodegradability, based on molecular fragments," *Chemosphere*, vol. 108, pp. 10-16, 8 2014.

[242] D. S. Katti, S. Lakshmi, R. Langer and C. T. Laurencin, "Toxicity, biodegradation and elimination of polyanhydrides," *Advanced Drug Delivery Reviews*, vol. 54, no. 7, pp. 933-961, 10 2002.

[243] K. I. Kasuya, K. I. Takagi, S. I. Ishiwatari, Y. Yoshida and Y. Doi, "Biodegradabilities of various aliphatic polyesters in natural waters," *Polymer Degradation and Stability*, vol. 59, no. 1-3, pp. 327-332, 1 1998.

[244] R. Jérôme and P. Lecomte, New developments in the synthesis of aliphatic polyesters by ring-opening polymerisation, Woodhead Publishing Limited, 2005, pp. 77-106.

[245] K. J. Jem and B. Tan, "The development and challenges of poly (lactic acid) and poly (glycolic acid)," *Advanced Industrial and Engineering Polymer Research*, vol. 3, no. 2, pp. 60-70, 4 2020.

[246] H. Greim, J. Ahlers, R. Bias, B. Broecker, H. Hollander, H. P. Gelbke, S. Jacobi,

H. J. Klimisch, I. Mangelsdorf, W. Mayr, N. Schön, G. Stropp, P. Stahnecker, R. Vogel, C. Weber, K. Ziegler-Skylakakis and E. Bayer, "Assessment of structurally related chemicals: Toxicity and ecotoxicity of acrylic acid and acrylic acid alkyl esters (acrylates), methacrylic acid and methacrylic acid alkyl esters (methacrylates)," *Chemosphere*, vol. 31, no. 2, pp. 2637-2659, 7 1995.

[247] H. Greim, J. Ahlers, R. Bias, B. Broecker, H. Hollander, H. P. Gelbke, S. Jacobi, H. J. Klimisch, I. Mangelsdorf, W. Mayr, N. Schön, G. Stropp, P. Stahnecker, R. Vogel, C. Weber, K. Ziegler-Skylakakis and E. Bayer, "Assessment of structurally related chemicals: Toxicity and ecotoxicity of acrylic acid and acrylic acid alkyl esters (acrylates), methacrylic acid and methacrylic acid alkyl esters (methacrylates)," *Chemosphere*, vol. 31, no. 2, pp. 2637-2659, 7 1995.

[248] H. Greim, J. Ahlers, R. Bias, B. Broecker, H. Hollander, H. P. Gelbke, S. Jacobi, H. J. Klimisch, I. Mangelsdorf, W. Mayr, N. Schön, G. Stropp, P. Stahnecker, R. Vogel, C. Weber, K. Ziegler-Skylakakis and E. Bayer, "Assessment of structurally related chemicals: Toxicity and ecotoxicity of acrylic acid and acrylic acid alkyl esters (acrylates), methacrylic acid and methacrylic acid alkyl esters (methacrylates)," *Chemosphere*, vol. 31, no. 2, pp. 2637-2659, 7 1995.

[249] G. Gorrasi and R. Pantani, "Hydrolysis and Biodegradation of Poly(lactic acid)," *Advances in Polymer Science*, vol. 279, pp. 119-151, 2017.

[250] D. Gamberger, D. Horvatić, S. Sekušak and A. Sabljić, "Applications of experts' judgement to derive structure-biodegradation relationships," *Environmental Science and Pollution Research*, vol. 3, no. 4, pp. 224-228, 1996.

[251] R. D. Fields, F. Rodriguez and R. K. Finn, "Microbial degradation of polyesters: Polycaprolactone degraded by P. pullulans†," *Journal of Applied Polymer Science*, vol. 18, no. 12, pp. 3571-3579, 1974.

[252] Dihora, "Shampoo compositions with increased deposition of polyacrylate microcapsules," 11 2014.

[253] K. Chrissafis, K. M. Paraskevopoulos and D. N. Bikiaris, "Effect of molecular weight on thermal degradation mechanism of the biodegradable polyester poly(ethylene succinate)," *Thermochimica Acta*, vol. 440, no. 2, pp. 166-175, 1 2006.

[254] P. Bhavsar, M. Bhave and H. K. Webb, "Effective multi-stage biodegradation of commercial bulk polyurethane by Clonostachys and Purpureocillium spp," *Science of The Total Environment*, vol. 908, p. 168329, 1 2024.

[255] C. R. Arza, P. Wang, J. Linares-Pastén and B. Zhang, "Synthesis, thermal, rheological characteristics, and enzymatic degradation of aliphatic polyesters with lignin-based aromatic pendant groups," *Journal of Polymer Science, Part A: Polymer Chemistry*, vol. 57, no. 23, pp. 2314-2323, 12 2019.

[256] N. R. Nair, V. C. Sekhar, K. M. Nampoothiri and A. Pandey, "Biodegradation of Biopolymers," 2017.

[257] J. Tunkel, P. H. Howard, R. S. Boethling, W. Stiteler and H. Loonen, "Predicting ready biodegradability in the Japanese ministry of international trade and industry test," *Environmental Toxicology and Chemistry*, vol. 19, no. 10, pp. 2478-2485, 10 2000.

[258] J. E. Potts, R. A. Clendinning, W. B. Ackart and W. D. Niegisch, "The

Biodegradability of Synthetic Polymers," *Polymers and Ecological Problems,* pp. 61-79, 1973.

[259] S. K. Saha and H. Tsuji, "Effects of molecular weight and small amounts of d-lactide units on hydrolytic degradation of poly(l-lactic acid)s," *Polymer Degradation and Stability,* vol. 91, no. 8, pp. 1665-1673, 8 2006.

[260] S. K. Saha and H. Tsuji, "Hydrolytic Degradation of Amorphous Films of L-Lactide Copolymers with Glycolide and D-Lactide," *Macromolecular Materials and Engineering,* vol. 291, no. 4, pp. 357-368, 4 2006.

[261] A. E. Rydholm, C. N. Bowman and K. S. Anseth, "Degradable thiol-acrylate photopolymers: polymerization and degradation behavior of an in situ forming biomaterial," *Biomaterials,* vol. 26, pp. 4495-4506, 2005.

[262] P. Vimala and L. Mathew, "Biodegradation of Polyethylene Using Bacillus Subtilis," *Procedia Technology,* vol. 24, pp. 232-239, 1 2016.

[263] C. G. Van Ginkel, A. Haan, M. L. Luijten and C. A. Stroo, "Influence of the Size and Source of the Inoculum on Biodegradation Curves in Closed-Bottle Tests," *Ecotoxicology and Environmental Safety,* vol. 31, no. 3, pp. 218-223, 8 1995.

[264] G. Thouand, B. Capdeville and J. C. Block, "Preadapted Inocula for Limiting the Risk of Errors in Biodegradability Tests," vol. 33, no. 3, pp. 261-267, 4 1996.

[265] J. R. A. Pires, V. G. L. Souza, P. Fuciños, L. Pastrana and A. L. Fernando, "Methodologies to Assess the Biodegradability of Bio-Based Polymers—Current Knowledge and Existing Gaps," *Polymers 2022, Vol. 14, Page 1359,* vol. 14, no. 7, p. 1359, 3 2022.

[266] H. A. Painter and E. F. King, "A respirometric method for the assessment of ready biodegradability: Results of a ring test," *Ecotoxicology and Environmental Safety,* vol. 9, no. 1, pp. 6-16, 2 1985.

[267] K. McDonough, G. Battagliarin, J. Menzies, J. Bozich, M. Bergheim, B. Hidding, C. Kastner, B. Koyuncu, G. Kreutzer, H. Leijs, Y. Parulekar, M. Raghuram and N. Vallotton, "Multi-laboratory evaluation of the reproducibility of polymer biodegradation assessments applying standardized and modified respirometry methods," *Science of The Total Environment,* vol. 901, p. 166339, 11 2023.

[268] K. McDonough, G. Battagliarin, J. Menzies, J. Bozich, M. Bergheim, B. Hidding, C. Kastner, B. Koyuncu, G. Kreutzer, H. Leijs, Y. Parulekar, M. Raghuram and N. Vallotton, "Multi-laboratory evaluation of the reproducibility of polymer biodegradation assessments applying standardized and modified respirometry methods," *Science of The Total Environment,* vol. 901, p. 166339, 11 2023.

[269] K. McDonough, N. Itrich, K. Casteel, J. Menzies, T. Williams, K. Krivos and J. Price, "Assessing the biodegradability of microparticles disposed down the drain," *Chemosphere,* vol. 175, pp. 452-458, 5 2017.

[270] Z. Majeed, N. K. Ramli, N. Mansor and Z. Man, "Starch Biodegradation in a Lignin Modified Slow Release Fertilizer: Effect of Thickness," vol. 625, pp. 830-833, 2014.

[271] S. Lv, Y. Zhang, J. Gu and H. Tan, "Soil burial-induced chemical and thermal changes in starch/poly (lactic acid) composites," vol. 113, pp. 338-344, 7 2018.

[272] P. Balakrishnan, V. G. Geethamma, S. Gopi, M. G. Thomas, M. Kunaver, M. Huskić, N. Kalarikkal, T. Volova, D. Rouxel and S. Thomas, "Thermal, biodegradation and theoretical perspectives on nanoscale confinement in starch/cellulose nanocomposite modified via green crosslinker," vol. 134, pp. 781-790, 8 2019.

[273] "Revised Introduction to the OECD Guidelines for Testing of Chemicals, Section 3," 9 2006.

[274] "OECD Guidelines for the Testing of Chemicals, Section 3 : Environmental fate and behaviour | OECD Guidelines for the Testing of Chemicals | OECD iLibrary".

[275] "D5338 Standard Test Method for Determining Aerobic Biodegradation of Plastic Materials Under Controlled Composting Conditions, Incorporating Thermophilic Temperatures".

[276] E. Besseling, P. Redondo-Hasselerharm, E. M. Foekema and a. A. A. Koelmans, "Quantifying ecological risks of aquatic micro- and nanoplastic," *Critical reviews in environmental science and technology,* vol. 49, pp. 32-80, 2019.

[277] J. Jaworska, S. Dimitrov, N. Nikolova and O. Mekenyan, "Probabilistic assessment of biodegradability based on metabolic pathways: CATABOL system," *SAR QSAR Environmental Research,* vol. 13, pp. 307-323, 2002.

[278] K. Bruyninckx and M. Dusselier, "Sustainable Chemistry Considerations for the Encapsulation of Volatile Compounds in Laundry-Type Applications," *ACS Sustainable Chemistry and Engineering,* vol. 7, no. 9, pp. 8041-8054, 5 2019.

[279] A. Jemec, P. Horvat, U. Kunej, M. Bele and A. Kržan, "Uptake and effects of microplastic textile fibers on freshwater crustacean Daphnia magna," *Environmental Pollution,* vol. 219, pp. 201-209, 12 2016.

[280] A. Lombardo, F. Pizzo, E. Benfenati, A. Manganaro, T. Ferrari and G. Gini, "New in silico classification model for ready biodegradability, based on molecular fragments.," *Chemosphere,* vol. 108, pp. 10-6, 2014.

[281] "OECD guideline for testing of chemical, Ready Biodegradability, Test 301," 1992.

[282] D. Baiocco, "Fabrication and characterisation of vegetable chitosan derived microcapsules," University of Birmingham, 2022.

[283] M. Wang, "A Deep Learning Model for Predicting Molecular Ready Biodegradability," P&G Technical report , 2019.

[284] "ISO 14855-1:2005 - Determination of the ultimate aerobic biodegradability of plastic materials under controlled composting conditions — Method by analysis of evolved carbon dioxide — Part 1: General method," 2005.

[285] "ISO 17556:2019 - Plastics — Determination of the ultimate aerobic biodegradability of plastic materials in soil by measuring the oxygen demand in a respirometer or the amount of carbon dioxide evolved," ISO, Geneva, 2019.

[286] "OECD guideline for testing of chemicals proposal for revised introduction to the OECD guidelines for testing of chemicals. Section 3 part 1: principles and strategies related to the testing of degradation of organic chemicals," 2005.

[287] "OECD guideline for testing of chemicals proposal for revised introduction to the

OECD guidelines for testing of chemicals. Section 3 part 1: principles and strategies related to the testing of degradation of organic chemicals," 2005.

[288] "Registration, Evaluation, Authorisation and Restriction of Chemicals (REACH), Regulation (EC) No 1907/2006 of the European Parlament and of the council," 2006.

[289] L. Feng, "Articles of manufacture with polyurea capsules cross-linked with chitosan". Patent WO2021163599, 2021.

[290] G. Sun and Z. Zhang, "Mechanical properties of melamine-formaldehyde microcapsules," *J. Microencapsulation,* vol. 18, pp. 593-602, 2001.

[291] Hirami and M. Mochizuki, "Structural Effects on the Biodegradation of Aliphatic Polyesters," *Polymers for Advanced Technologies,* vol. 8, p. 203–209.

[292] L. T. Isabelle Vroman, "Isabelle Vroman and Lan Tighzert," *Materials,* vol. 2, pp. 307-344, 2009.

[293] H. Ibrahim, S. Mehanny, L. Darwish and M. Farag, "A Comparative Study on the Mechanical and Biodegradation Characteristics of Starch-Based Composites Reinforced with Different Lignocellulosic Fibers," *Journal of Polymers and the Environment,* vol. 26, p. 2434–2447, 2018.

[294] K. XY, L. XY and W. XH, "Synthesis and characterization of a novel MPEG-chitosan diblock copolymer and self-assembly of nanoparticles.," *Carbohydr Polym,* p. 170–5, 2010.

[295] C. K. S. Pillai, W. Paul and C. P. Sharma, "Chitin and chitosan polymers: Chemistry, solubility and fiber formation.," in *Progress in Polymer Science*, 2009, p. 641–678.

[296] R. Arshady, "Preparation of microspheres and microcapsules by interfacial polycondensation techniques.," *J Microencapsul,* p. 6:13–28, 1989.

[297] H. B. Scher, Microencapsulated Pesticides, 1977, pp. 126-144.

[298] D. Elieh-Ali-Komi and M. R. Hamblin, "Chitin and Chitosan: Sources, Production and Medical Applications," pp. 292-318, 2011.

[299] V. S and T. I. V., "Modeling the Biodegradability of Chemical Compounds Using the Online CHEmical Modeling Environment (OCHEM).," *Mol Inform,* vol. 33(1), pp. 73-85, 2014.

[300] "Opinion on solubility of Synthetic Amorphous Silica (SAS)," Scientific Committee on Consumer Safety, 2019.

[301] P. Agamuthu and P. N. Faizura, "Biodegradability of degradable plastic waste," vol. 23, no. 2, pp. 95-100, 4 2005.

[302] M. Roth, Y. Matsumoto and H. Blauer, "Process for the production of acrylic acid esters containing carboxyl groups". Patent WO2005030696A1, 9 2004.

[303] O. S. Alimi, J. Farner Budarz, H. L. M. and N. Tufenkji, "Microplastics and Nanoplastics in Aquatic Environments: Aggregation, Deposition, and Enhanced Contaminant Transport.," *Environmental Science and Technology,* vol. 52, pp. 1704-1724, 2018.

[304] European Chemicals Agency (ECHA), "Annex XV Restriction report," Helsinki, Finland, 2019.

[305] "ASTM D5988-18 - Standard Test Method for Determining Anaerobic Biodegradation of Plastic Materials Under High-Solids Anaerobic-Digestion Conditions," ASTM, 2018.

[306] W. Conshohocken, Ed., ASTM D5338-15 - Standard Test Method for Determining Aerobic Biodegradation of Plastic Materials under Controlled Composting Conditions, Incorporating Thermophilic Temperatures, PA: ASTM International, 2015.

[307] "ISO 18830:2016 Plastics - Determination of aerobic biodegradation of non-floating plastic materials in a seawater/sandy sediment interface - Method by measuring the oxygen demand in closed respirometer," ISO, Geneva, 2016.

[308] "ISO 19679:2020 - Plastics — Determination of aerobic biodegradation of non-floating plastic materials in a seawater/sediment interface - Method by analysis of evolved carbon dioxide," ISO, Geneva, 2016.

[309] OECD, "OECD 314 Simulation Tests to Assess the Biodegradability of Chemicals Discharged in," OECD Guidelines for the Testing of Chemicals, 2008.

[310] H. K. No, N. Y. Park, S. H. Lee and S. P. Meyers, "Antibacterial activity of chitosans and chitosan oligomers with different molecular weights," in *International journal of Food Mircrobiology*, 2002, pp. 74(1–2), 65–72.

[311] D. Poncelet, E. Teunou, A. Desrumaux and D. D. Valle, "Emulsification and microencapsulation: State of the art," *Landbauforschung Volkenrode,* vol. SH 241, no. 27-31, 2002.

[312] A. Martin, Biodegradation and bioremediation, Academic Press, 1999.

[313] B. K. ,. Richard A. Gross, "Biodegradable Polymers for the Environment," *Science*, no. 297, pp. 803-807, 2002.

[314] R. R. R Chandra, "Biodegradable polymers," *Progress in Polymer Science*, vol. 23, no. 7, pp. 1273-1335, 1998.

[315] T. &. C. C. &. M. G. &. L. M. Roychowdhury, "The Surface Analytical Chemistry (XPS) and Polymer Chemistry of the Acrylates and Methacrylates, an Introduction," *Vacuum Technology and Coatin*, 2015.

[316] J. Dihora and S. W. J. W. Jonathan Cetti, "Spray drying microcapsules". Patent WO2014047486, 2013.

[317] T. A. Khan, K. K. Peh and H. S. Ch'ng, "Reporting degree of deacetylation values of chitosan: the influence of analytical methods," *J Pharm Pharmaceut Sci*, 2002.

[318] T. Ohara, T. Sato, N. Shimizu, G. Prescher, H. Schwind, O. Weiberg, K. Marten, H. Greim, T. Shaffer and P. & Nandi, "Acrylic acid and derivatives," *Ullmann's Encyclopedia of Industrial Chemistry*, 2020.

[319] S. Schwarzer and U. Hoffmann, "Experimental Reaction Equilibrium and Kinetics of the Liquid-phase Butyl Acrylate Synthesis Applied to Reactive Distillation Simulations," *Chemical Engineering & Technology,* vol. 25, no. 10, pp. 975-980, 2002.

[320] J. Salaklang, V. Maes, M. Conradi, R. Damsb and T. Junkers, "Direct synthesis of acrylate monomers in heterogeneous continuous flow processes," *Reaction Chemistry & Engineering,* vol. 3, pp. 41-47, 2018.

[321] M. Roth, Y. Matsumoto and H. Blauer, "Process for the production of acrylic acid esters containing carboxyl groups". Patent WO2005030696A1, 2004.

[322] Y. Gao, D. Zhao, M.-W. Chang, Z. Ahmad and J.-S. Li, "Optimising the shell thickness-to-radius ratio for the fabrication of oil-encapsulated polymeric microspheres," *Chemical Engineering Journal*, vol. 284, pp. 963-971, 2016.

UNIVERSITAT ROVIRA I VIRGILI
NEW METHODOLOGIES FOR ENVIRONMENTALLY FRIENDLY MICROCAPSULE DESIGN
Mattia Collu